Marine and Petroleum Geology 113 (2020) 104176

Contents lists available at ScienceDirect

Marine and Petroleum Geology

journal homepage: www.elsevier.com/locate/marpetgeo

Research paper

Facies classification and patterns of lacustrine carbonate deposition of the Barra Velha Formation, Santos Basin, Brazilian Pre-salt

J.P. Gomes[a,b,*], R.B. Bunevich[b], L.R. Tedeschi[b], M.E. Tucker[a], F.F. Whitaker[a]

[a] School of Earth Sciences, University of Bristol, Queens Road, Bristol BS8 1RJ, England, UK
[b] Reservoir Team, Petrobras S. A., Centro Empresarial Senado, 7, andar, Torre B, Avenida Henrique Valadares, 28, Centro, Rio de Janeiro, 20231-030, Brazil

ARTICLE INFO

Keywords:
Facies classification
Pre-salt deposits
Lacustrine carbonate
Spherulites
Shrubs

ABSTRACT

The lacustrine carbonate rocks of the giant Pre-salt oil-fields in the Santos and Campos Basins differ in a number of important aspects from classic lake deposits. Prior work has described distinctive and unusual features of deposition, early diagenesis and reservoir quality with in these rocks that defy classification using established schemes. In addition to their unusual textures, debate continues as to how to interpret the vertical stacking pattern of facies. A new facies classification scheme is proposed based on the relative abundance of three end-member components: mud (micrite and clay minerals), calcite spherulites and fascicular calcite shrubs. Although focused on the main textural and mineralogical features of the rocks as seen today, the proposed scheme takes into account the relative contribution of depositional and early diagenetic components, sediment mineralogy and the degree of dissolution. Application of this scheme offers insight into depositional conditions, whilst also linking to reservoir quality. Basic (elementary) cycles can be defined using this classification in combination with the variation in the abundance of detrital grains and the chemical composition. Three possible models are suggested to interpret the origin of the basic cycle within the Barra Velha Formation in the context of variation in climate, lake level and water chemistry. Integration of data from different sources, including petrographic, core description and chemical data for the basic cycle, offers improved process-based understanding of metre-scale facies patterns and provides a foundation for understanding larger scale vertical variations within and between unconformity-bound sequences.

1. Introduction

Geological understanding of carbonate facies has improved over the last few decades, particularly our appreciation of biological and diagenetic processes and their products. A facies classification scheme has four functions (Walker, 1992): characterizing a sediment/sedimentary rock; integrating facts and observations to facilitate interpretation of the environment of deposition; providing a norm for purposes of comparison, and acting as a framework to direct further observations. However, the main reason to use a classification, apart from giving a rock a name, is to communicate information concerning the features of a rock. The chosen names may be arbitrary or have some level of overlap with an existing classification, but critically they should be precisely defined to improve the discussion of characterization and interpretation.

Following these principles, several classifications for carbonate rocks have been proposed. The genetic classification of limestones introduced by Folk (1959, 1962) is based on the presence or absence of matrix (micrite) versus cement (sparite), plus a prefix to indicate the dominant grains present (allochems: bio-oo- pel- or intra-), to give the limestone a simple descriptive name. The more texturally-based Dunham (1962) classification uses the amount of lime mud and abundance of grains, which reflect the energy level in the environment, to group limestones into four main categories: grainstone, packstone, wackestone and mudstone – with boundstone for reefal and microbial limestones. To recognize particular types of boundstone within reefal rocks, Embry and Klovan (1971) suggested the terms framestone, baffestone and boundstone. Similarly, Riding (2000) recognized four types of microbialite: stromatolite, thrombolite, dendrite and leiolite. For a limestone dominated by a cement, Wright (1992) proposed the term cementstone.

Some of these classifications, originally conceptualized for marine carbonates, have been used for lacustrine deposits with some modifications and variable degrees of success (Walker, 1992). However, the lacustrine carbonate rocks of the giant Pre-salt oil-fields in the Santos and Campos Basins, offshore Brazil, differ in a number of important

* Corresponding author. School of Earth Sciences, University of Bristol, Queens Road, Bristol BS8 1RJ, England, UK.
E-mail address: jpgomes@petrobras.com.br (J.P. Gomes).

https://doi.org/10.1016/j.marpetgeo.2019.104176
Received 25 September 2019; Received in revised form 4 December 2019; Accepted 11 December 2019
Available online 16 December 2019

aspects from classic well-documented carbonate lake deposits. 1) The configuration of Cretaceous horsts and grabens generated many islands surrounded by an extensive lake, or many small lakes with variable connectivity through time (Pietzsch et al., 2018). 2) The siliciclastic lake shoreline is located far to the west from the areas of hydrocarbon exploration interest (Dias, 2005). 3) Carbonate deposits appear to be laterally continuous over tens of kilometres (Carminatti et al., 2008). 4) The carbonates are comprised of three main components and detrital material derived from them: shrubs, millimetre-scale fibrous laminae and spherulites (Wright and Barnett, 2015).

Published articles describing these Pre-salt deposits have tried to fit them within pre-existing facies schemes (Wright and Barnett, 2015; Muniz and Bosence, 2015; Wright and Barnett, 2017; Herlinger et al., 2017, Liechoscki de Paula Faria et al., 2017; Arienti et al., 2018; Artagão, 2018; Sartorato, 2018; Farias et al., 2019; Tanaka et al., 2018; Lima and De Ros, 2019; Wright and Barnett, 2019). However, this has given rise to a confusing range of terms to describe a single rock fabric. For example, a rock composed of shrub-like calcite crystals has been classified variously as a stromatolite and a thrombolite (Terra et al., 2010; Muniz and Bosence, 2015), as fascicular calcite crust (Herlinger et al., 2017; Lima and De Ros, 2019) or as *in situ* shrubs (Wright and Barnett, 2015) or shrub-like facies (Farias et al., 2019). Similarly, rocks composed of spherulites have been classified as spherulite-dominated lithologies (Wright and Barnett, 2015), as Mg-clay with spherulites facies and spherulitite (Farias et al., 2019) and as stevensitic claystones with calcite spherulites (Lima and De Ros, 2019). In contrast, the abundant fine-grained facies are widely described as laminites (Lima and De Ros, 2019; Muniz and Bosence, 2015). There has been considerable discussion about the way in which established terminology to describe facies can best be applied in a Pre-salt context. In many cases these terms are associated with distinct paleoenvironmental conditions and/or formation processes. There is a clear need for a facies classification scheme based on the proportion of components that characterizes the lacustrine sediments of the Pre-salt and that is distinct from a process-based classification, and thus can help evaluate alternative models of formation. Any such scheme should also allow evaluation of the variability of these components on a micro- and macroscale in order to understand variations through the stratigraphic succession and to allow a proper facies upscaling.

Our objective in this paper is to propose a new facies classification scheme in order to document, in a more meaningful manner, the vertical trends in sediment texture and composition for the lacustrine carbonates of the Pre-salt Barra Velha Formation in our area of study of the Santos Basin (Fig. 1). This is based on the textural and mineralogical features of the rocks as seen today, and considers the relative abundance of the three end-member components that are formed *in situ*: mud (dolomite, calcite, silica and Mg-clay), calcite spherulites and fascicular calcite shrubs. In addition, the proposed scheme takes into account the relative contribution of depositional and early diagenetic components, sediment mineralogy and the degree of dissolution, as well as any reworking of *in-situ* sediment. Although developed for the database of Barra Velha Formation, we believe this scheme may have wider application in supporting systematic and consistent descriptions and interpretations of deposits from both Barra Velha Formation from other pre-salt areas and a range of comparable alkaline lake systems with similar facies. It is worth to mention that our area of study does not include all facies described in other areas, such as the microbial silicified boundstone in Kwanza Basin (Saller et al., 2016). As an example of the application of the new facies scheme, the occurrence of the various facies types is combined with the abundance of detrital grains and trace element variations to characterize metre-scale ideal cycles within the Barra Velha succession and to propose alternative process-based models of changes in the environment of deposition.

2. Geological setting

The southern domain of the South Atlantic is composed of a number of extensive basins, which include the Santos and Campos basins offshore Brazil (Fig. 1A) and the Kwanza and Namibe basins offshore southwest Africa. These have been interpreted as resulting from two phases of extension during the pre-rift stage of South Atlantic opening in the Late Hauterivian–Early Barremian. The succeeding rift phase in the later Barremian-Aptian lasted 5–6 My and was characterized by tilting of fault-blocks and growth strata in upper continental crust, followed by the development of a flexural and continuous sag basin (Chaboureau et al., 2013). The Santos Basin is located on the southeastern Brazilian margin, between the Campos Basin in the north and the Pelotas Basin in the south, east of the Brazilian states of São Paulo and Rio de Janeiro (Fig. 1B). It is one of the most extensive offshore brazilian basins, with an area of 352,000 km^2, and a current water depth of up to 3,000 m. The main structural features are the Cabo Frio High to the northeast, the Florianópolis Platform to the southwest, the Santos hinge line to the west, which marks the external (western) limit of the salt (Ariri Formation), and the São Paulo plateau to the east. Our area of interest is located in region of the Santos Outer High in the central part of the Santos Basin (Fig. 1C). Liechoscki de Paula Faria et al. (2017) performed a restoration from balanced cross-sections and concluded that this area of the Santos basin did not undergo structure inversion, which implies the actual structure high was also a palaeohigh throughout Barra Velha deposition.

The basement of the Santos Basin is composed of Precambrian metamorphic rocks. Tholeiitic flood basalt formed during the early stages of rifting in the Lower Cretaceous (Camburiú Formation), is the equivalent of the Cabiúnas Formation in the Campos Basin and it has been dated to 134–122 Ma (Mizusaki et al., 1992). The sediments of the Santos Basin (Fig. 2) are divided into three super-sequences: rift, post-rift and drift (Moreira et al., 2007). The rift super-sequence is composed of continental siliciclastics, talc-stevensite ooids with interbedded lacustrine coquinas and organic-rich shales of the Piçarras and Itapema formations. This was followed by a post-rift super-sequence, comprising lacustrine carbonates and shales of the Barra Velha Formation, which is followed by evaporitic deposits of anhydride and halite, locally with more soluble salts such as carnallite, sylvite and tachyhydrite, forming the Ariri Formation. Three major unconformities are important for understanding the Barra Velha Formation: the basal Pre-Alagoas Unconformity (PAU) at the top of the coquina deposits, an internal unconformity called the Intra-Alagoas Unconformity (IAU), and the Salt Base Unconformity (SBU) that caps the formation (Fig. 2). Finally, the basin evolved into a passive-margin basin with an early drift supersequence represented by shallow-marine platform carbonates of the Guarujá Formation, followed by platform drowning and deeper-water sediments of the Itanhaém Formation.

High-frequency basic (ideal or elementary) cycles, consisting of a regular repetition of facies, have been recognized in these lacustrine carbonates in the Santos and Campos basins (Dias, 2005; Wright and Barnett, 2015; Muniz and Bosence, 2015; Liechoscki de Paula Faria et al., 2017; Arienti et al., 2018; Artagão, 2018; Sartorato, 2018; Farias et al., 2019; Lima and De Ros, 2019). The basic cycles are represented as having a thickness of 1–2 m, although examples range from 0.75 to 5 m. These cycles typically are comprised of mud-grade laminated carbonates, followed by units containing millimetre-diameter spherulites, and finally units dominated by millimetre–centimetre calcitic crystal shrubs (Wright and Barnett, 2015). These authors interpreted mudstone-claystone-laminite facies to have formed in the relatively deep-water part of the lake. The shrubs formed on the floor of the lake, in many cases followed by subaerial exposure, and the generation of breccias, suggesting deposition in shallow water or during a period of shallowing. Whilst there is general agreement over the character of the proposed cycles, there is still intense debate about many aspects of these Barra Velha sediments. These include the biological or abiotic

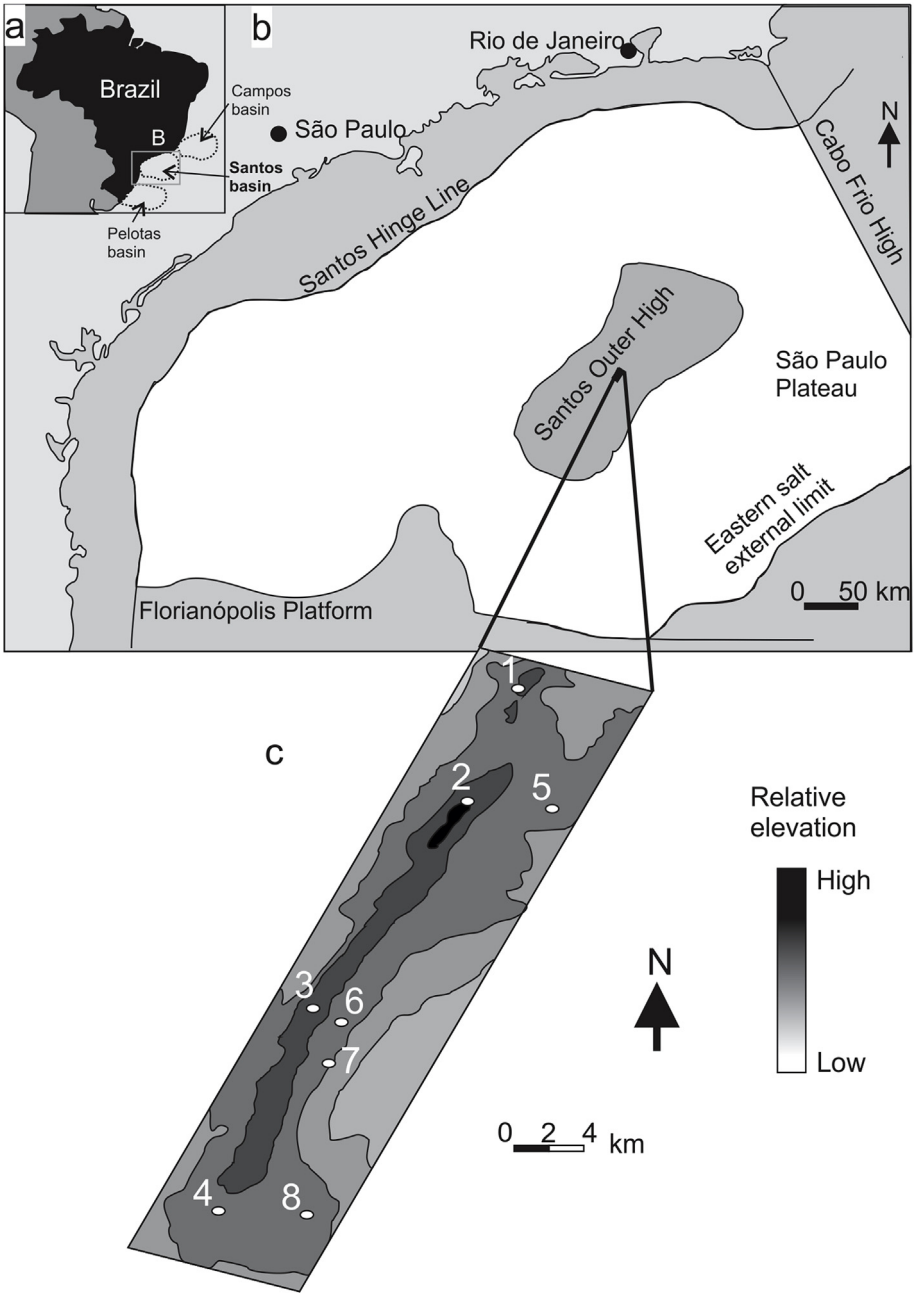

Fig. 1. Location of the Santos and Campos Basins, South Atlantic, offshore Brazil, with the white area representing the basin boundaries (A). Area of interest within the region of the outer high of the Santos Basin (B), with location of the wells examined (C). Modified from Melo Garcia et al. (2012).

origin of most of the facies, whether the spherulites are primary or early diagenetic and the composition of the associated fine grains, some of which were subsequently dissolved (organic matter related to extracellular polymeric substances or magnesium clay minerals). Our work and that of others (Dias, 2005; Wright and Barnett, 2015; Muniz and Bosence, 2015; Arienti et al., 2018; Artagão, 2018; Sartorato, 2018; Farias et al., 2019; Lima and De Ros, 2019) suggests that in fact there are other types of basic cycle with different facies associations.

3. Materials and methods

This paper focuses on data from eight wells distributed along the horst structure of the Santos Outer High (Fig. 1C). The cores available mostly come from the upper section of the Barra Velha Formation above the Intra-Alagoas Unconformity, with additional material from sidewall cores taken from the lower section (Fig. 3).

Core was recovered from six wells, with extended core from two sites (wells 3 and 2) spanning 197 m and 93 m respectively, whereas at the other sites core lengths were 30 m, 12 m, 30 m and 27 m (Fig. 3), totalizing 389 m of described core. For two wells (7 and 8) only sidewall cores are available. 778 sidewall cores and 1143 plugs were prepared from blue epoxy resin-impregnated samples. Samples were stained with Alizarin red-S and potassium ferricyanide solution to aid the identification of carbonate minerals as outlined by Dickson (1966). All thin-sections were examined by petrographic microscope and the relative abundance of components was determined for all samples. Quantitative petrography was performed on 10 representative thin-sections by counting 200 points per sample to evaluate the texture of the carbonate grains, and diagenetic constituents.

The methodology used by Muniz and Bosence (2015) to interpret

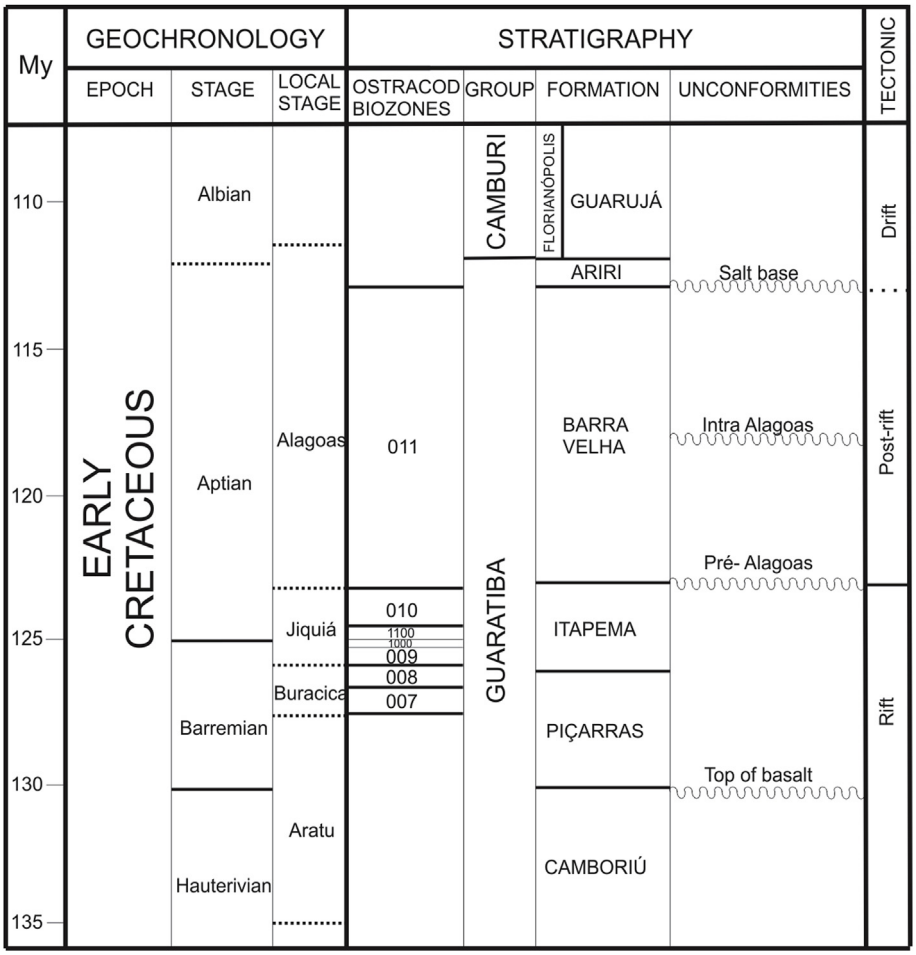

Fig. 2. Lower Cretaceous stratigraphic chart for the Santos Basin (adapted from Moreira et al., 2007) and ostracod biozones (modified from Pietzsch et al., 2018). The present study focusses on the Barra Velha Formation, which is bounded by the Pre-Alagoas and Salt Base unconformities and separated into the Lower and Upper Barra Velha Formation by the Intra-Alagoas Unconformity. The Barra Vellha Formation was deposited during the Alagoas local stage, which is correlated to ostracod biozone 011 and broadly to the Aptian (Moreira et al., 2007).

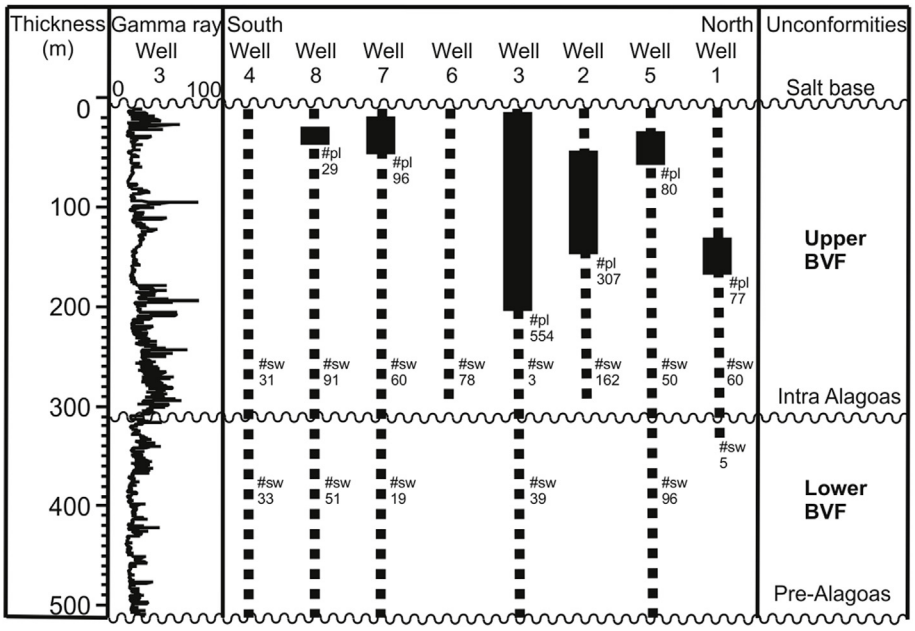

Fig. 3. Sample distribution within the Barra Velha Formation, which is ~500 m thick in the studied area. Cores are available from the upper Barra Velha Formation of six out of 8 wells (thick bars) and sidewall cores from below (dashed intervals). The numbers of thin sections of plugs from cores and sidewall cores are also shown, in which thin sections from sidewall cores from Lower and Barra Velha Formation are also represented below and above Intra-Alagoas unconformity. The gamma ray data are from Well 3 and are shown in API. BVF= Barra Velha Formation, #sw = number of side wall cores, #pl = number of plugs.

the facies from Formation Image Logs (FMI Log) for the intervals without cores, was applied create a qualitative facies log based on the sidewall-core facies and differences in image texture. Wireline logs (gamma ray especially) and thin-sections from sidewall-core samples were used as additional data in order to determine and interpret the facies.

Quantitative Evaluation of Minerals by SCANning electron microscopy (QEMSCAN) and X-Ray Diffraction (XRD) data were also obtained for different facies. Chemical and mineralogical maps of 10 representative thin-sections were produced using a QEMSCAN 650 automated mineralogical mapping instrument with accelerating voltage of 15 kV and 10 μm spot size. The mineralogical maps show the spatial distribution of mineral phases and the relationship between them; their abundance was quantified as area percentages or percentage of mass (considering the theoretical density of minerals). Quantities lower than 0.01% were ignored. Chemical analysis was performed on 590 samples from Well 3 core samples using ICP-OES (Inductively Coupled Plasma Optical Emission Spectrometry) in order to determine the elemental abundance of Al_2O_3, Fe_2O_3, CaO, Cr_2O_3, K_2O, MgO, MnO, Na_2O, SiO_2 and TiO_2. Most analytical chemical data are of a closed form, where individual components are summed, yielding an identical total. As result, as some elements increase in relative abundance others must decrease. This aspect leads to correlation measures and graphical presentations that do not reflect the true underlying relationships. This constraint can be corrected before multivariate statistical analysis by making a centred log-ratio transformation (CLR) as described by Montero-Serrano et al. (2010). The chemical data after CLR and the detrital grain abundance from XRD data were interpreted using Principal Component Analysis (PCA) to understand the correlation between these variables. Finally, vertical variations in facies, detrital content and elemental composition were used qualitatively to identify the basic cycles.

4. Facies classification

The Barra Velha facies samples from the eight wells are dominated by variable amounts of three components that were formed *in situ*: mud understood as fine-grained components (microcrystalline calcite and clay minerals), calcite spherulites and fascicular-optic calcite shrubs. These have been described in previous studies of Pre-salt carbonates in the Santos and Campos basins, as well as from the Namibian and Kwanza basins. However, there is a lack of consensus as to the processes responsible for formation of some of these components. Here we describe the main component grains in our study area and propose a new facies classification.

4.1. Description of main components

Mud: The fine-grained material in the Pre-salt carbonates, as matrix between grains and as beds, is broadly referred to as mud. This includes that comprised of clay minerals, calcite, dolomite and silica. Petrographically the clays occur as optically clear grains of clay aggregates, usually within beds which are massive or have a fine millimetric-scale lamination (examples of these are shown in Fig. 4). The clay minerals may show a degree of replacement by microcrystalline dolomite and microcrystalline silica. In other cases, the fine-grained sediment is micrite, which is mostly composed of calcite but may show a degree of replacement by dolomite and silica. Some of the dolomite/silica could be primary, but likely formed via a metastable precursor. In general, the light cream to dark brown coloured sediments show a plane-parallel to smooth wavy lamination, with thicknesses varying from millimetres to centimetres (examples of these are shown in Fig. 5). Optical microscopy shows that the light laminae are composed of microcrystalline calcite and the dark bands are composed of microcrystalline and rhombohedral dolomite and organic matter. Some mud samples contain fine siliciclastic grains, ostracods and phosphatic particles (Fig. 5). The main clay minerals present in the Barra Velha Formation are kerolite, stevensite, saponite, sepiolite, illite and mixed-layer minerals kerolite/smectite and illite/smectite (Souza et al., 2018; Madrucci et al., 2019).

Spherulites: The spherulites are spherical to sub-spherical calcite aggregates with radial extinction that commonly are dolomitized or recrystallized. Spherulites from ten thin sections were measured and range in diameter from 0.1 mm to 4 mm, with a mean of 1 mm (± 0.3 standard deviation, n = 800), and a mode of 0.6 mm (Figs. 6c–h and 7). The low variance in their size distribution suggests the same process of formation for all spherulites. A notable exception is the small number of samples (n = 3) that show normal or inverse grading at the thin-section scale, suggesting a relationship between spherulite size and an ideal combination of water chemistry and hydrodynamic conditions. In some cases, it is possible to recognize nuclei composed of cryptocrystalline micrite, clay minerals and, more rarely, a fragment of ostracod. The calcitic fibro-radial texture is preserved in most of the samples, but chalcedonic and micro-quartz replacement locally results in the loss of original fabric. Some spherulites are asymmetric, with preferential growth in one particular direction. In most cases, spherulites tend to grow upwards, whereas in some layers the spherulites grow parallel to the bedding. Some grains are a mixture of a fascicular component similar to a shrub and yet show a fibro-radial texture characteristic of a spherulite. In these situations, the volumetrically dominant of the two textures is used to determine the component name.

Shrubs: The term shrub is applied in this study to the 'ray crystal crust' defined by Folk et al. (1985), emphasizing the morphological similarity to fascicular-optic calcite (*sensu* Kendall, 1977) with a divergent optic-axis pattern within each crystal away from the substrate. Shrubs are composed of fibrous to extremely coarse bladed calcite crystals, with the long axis of their fan-shaped structure ranging from 0.15 to 6.5 mm in length. Some shrubs incorporate random fine detrital grains or, rarely, bioclasts within their structure. Within an individual layer, shrubs are oriented parallel to one another, varying from densely packed (0.2 mm between shrub central axes) to widely spaced (4 mm spacing) (Fig. 6 a and b). In some samples it is possible to identify more than one growth phase, resulting in a composite shrub that extends up to 20 mm. The shrubs occur predominantly as horizontal layers and locally form low domal structures (Terra et al., 2010; Wright and Barnett, 2015; Rezende and Pope, 2015).

4.2. Facies classification

The triangular diagram (Fig. 8) shows the proposed classification that encapsulates the range of combinations of the three main components where there is no evidence of significant reworking. The most abundant component gives a rock name, and the secondary component provides a qualifying adjective. Figs. 4–6 show thin-section examples of each facies type defined. In addition, an adjective for the main diagenetic event can be added, for example dolomitic spherulitestone (Fig. 6 g and h), silicified spherulitestone or dissolved spherulitestone.

In order to provide sufficient categories to differentiate rocks of significantly different composition, the classification triangle for *in situ* deposits (Fig. 8) is subdivided into nine rock types. The percentage values selected for the boundaries are those that provide a convenient separation of common combinations described in cores and thin-sections. In the classification of an essentially continuous series, all divisions are arbitrary (Folk, 1959). The boundaries used in the proposed classification unavoidably reflect personal opinion, but it is suggested they coincide with a separation of components formed by different processes.

The *in situ* carbonates comprising more than 90% of shrubs, spherulites or mud-rich end-members are designated shrubstone, spherulitestone and mudstone respectively (Fig. 8). The combination of more than 50% shrubs and less than 10% mud separates spherulitic shrubstone from shrubby spherulitestone. Rocks with more than 10%

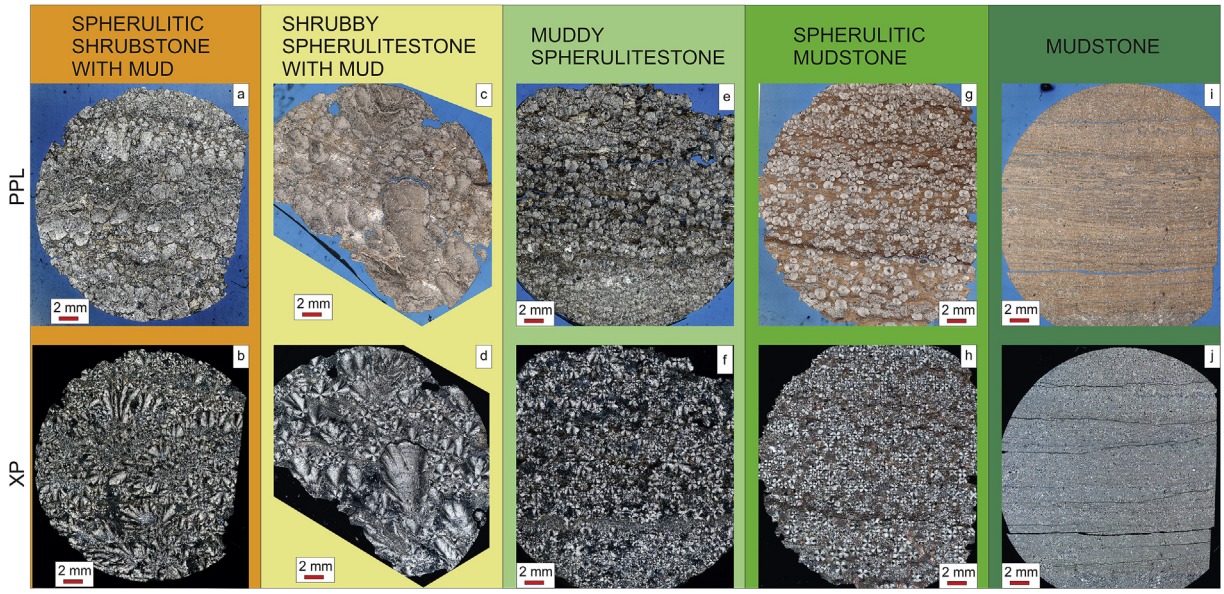

Fig. 4. Facies classification: a) and b) spherulitic shrubstone with mud, comprising calcite shrubs, calcite spherulites and Mg-clays locally replaced by dolomite; c) and d) shrubby spherulitestone with mud, comprising fascicular calcite shrubs, calcite spherulites and Mg-clays; e) and f) muddy spherulitestone, comprising calcite spherulites and Mg-clays; g) and h) spherulitic mudstone, comprising calcite spherulites and Mg-clays; i) and j) Mg-clay mudstone. All images pairs are PPL and XP and were impregnated with blue epoxy resin to highlight the porosity. (For interpretation of the references to colour in this figure legend, the reader is referred to the Web version of this article.)

mud are divided according to the proportion of the two components. Spherulitic shrubstone with mud and shrubby spherulitestone with mud are divided by the 50% shrub content. A rock with less than 10% shrubs is divided according to mud and spherulite proportions into muddy spherulitestone if the proportion of spherulites is higher than 70% and spherulitic mudstone otherwise. The term mudstone is applied to all samples that comprise > 90% fine-grained (< 64 μm) components. These components include Mg-clays, microcrystalline calcite, microcrystalline dolomite, and microcrystalline silica, and the nature of the fine-grained component can be specified by adding an adjective (Mg-clay, calcitic, dolomitic or siliceous mudstone). There is an intense debate about origin of each of these components in the Pre-salt, as discussed below, and thus the proposed classification scheme adopts a pragmatic approach to distinguish the facies as they occur/are today.

Sedimentary processes can fragment and transport the carbonate components that formed *in situ*, generating a new, reworked facies type. These reworked facies are composed of intraclasts (fragments of shrubs and spherulites), with grain-size varying from fine to very coarse, moderate to poor sorting, and massive to cross-stratified units. Bed thickness ranges from several cm up to 2 m. These facies can be classified using the Dunham (1962) scheme (Figs. 9 and 10). We suggest that where reworked components are dominant (> 50%) then this terminology should be used, but where they represent < 50%, then the facies descriptions based on *in situ* components are more appropriate. In the rare instances that include mud intraclasts (120 of 1921 thin-sections) or volcanic fragments (17 of 1921 thin-sections) additional qualifying adjectives can be added (intraclastic and volcanoclastic respectively).

The degree to which muddy facies are *in situ* or redeposited can be difficult to determine without reference to sedimentary structures, and hence the term mudstone is used for both. What can be more easily determined is the mineralogy of the mudstone facies, which can comprise silica, Mg-clay minerals, micrite and/or dolomite. Where it is possible to determine the mineralogy, the terms siliceous mudstone, calci-mudstone, dolo-mudstone and Mg-clay mudstone can be used, with mixed mudstone indicating no one component is dominant (> 50%) (Fig. 10). In addition, the adjective laminated can be added where it is possible to identify lamination. The introduction of the

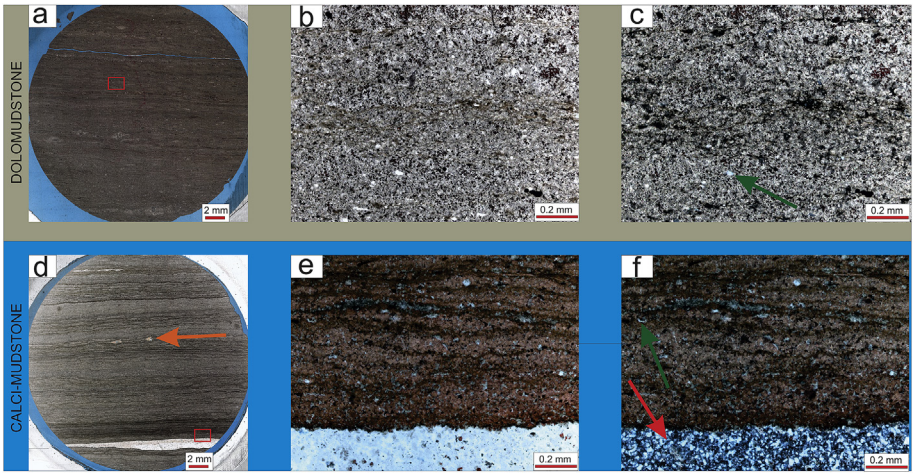

Fig. 5. a to c show dolo-mudstone where dolomite has replaced original calcite. Green arrow in c points to fine grain of detrital quartz; d to f show calci-mudstone. Orange arrow in d shows phosphate particle. Green arrow in f points to fine grain of detrital quartz. Red arrow in f points to a level where calcite is replaced by chalcedonic quartz. Samples b, c, e and f were stained with Alizarin red S. a, b, c and d are PPL and e and f are XP. Al images were impregnated with blue epoxy resin to highlight the porosity.

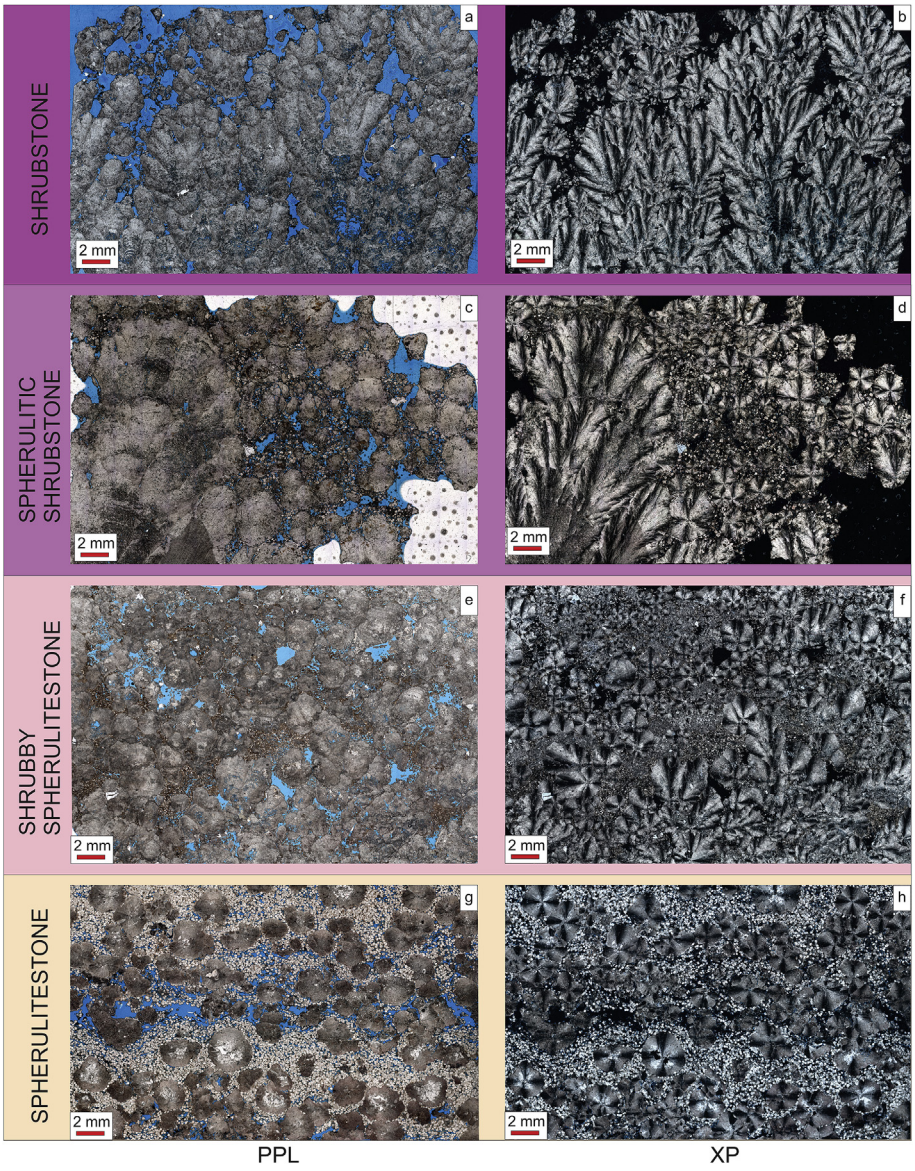

Fig. 6. Facies classification: a) and b) shrubstone, comprising fascicular-optic calcite crust with framework porosity; c) and d) spherulitic shrubstone, comprising fascicular optic shrubs, calcite spherulites and microcrystalline dolomite with inter-particle porosity; e) and f) shrubby spherulitestone, comprising fascicular optic shrubs, calcite spherulites and microcrystalline dolomite with inter-particle porosity; g) and h) spherulitestone, comprising calcite spherulites and rhombohedral dolomite with inter-particle porosity. All image pairs are PPL and XP and were impregnated with blue epoxy resin to highlight the porosity. (For interpretation of the references to colour in this figure legend, the reader is referred to the Web version of this article.)

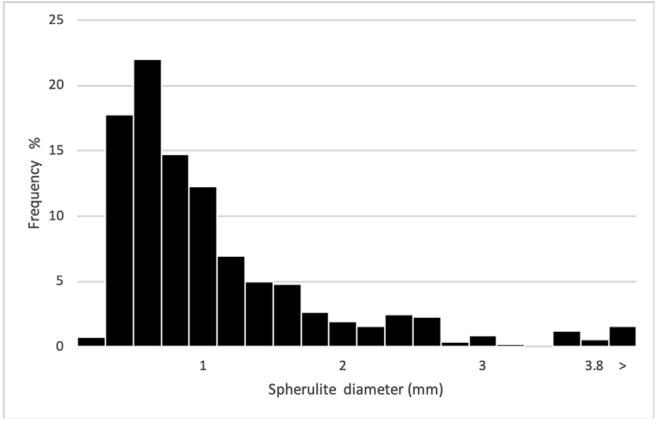

Fig. 7. Distribution of spherulite diameter measured in 563 spherulites from 10 thin-sections. The log-normal distribution has a mean value of 1 mm and standard deviation of 0.8 mm, and a mode of 0.6 mm.

mineralogical qualifier can be added before the word mud, such as spherulitestone with dolomitic/calcitic/siliceous mud in cases where this will help in the description.

We thus propose a set of three triangular diagrams to cover all the facies recognized from the Barra Velha Formation (Fig. 10), separated into in-situ and reworked facies. Mudstone may be *in situ* or reworked, and this is further classified according to mineralogical composition. Travertine has been rarely described from the BVF (Falcao, 2015; Souza et al., 2018) and for these accepted classification schemes (Pentecost and Viles, 1994; Erthal et al., 2017) should be used. Some workers have described microbialites from the BVF, specially for "Lula fingers" and for such deposits classification schemes are available (Riding, 2000; Terra et al., 2010).

The proposed classification is based on the textures identified in the present-day samples, with the objective of giving a clearer understanding of the facies distribution and linking this with reservoir quality. There are a number of ways in which this new facies classification scheme can be used. Here we illustrate its application to recognize facies cycles and implications for the processes generating elementary cycles. In addition, the classification scheme can provide a basis to examine the variations in diagenesis, vertically and laterally through the succession, as well as to compare the facies patterns with

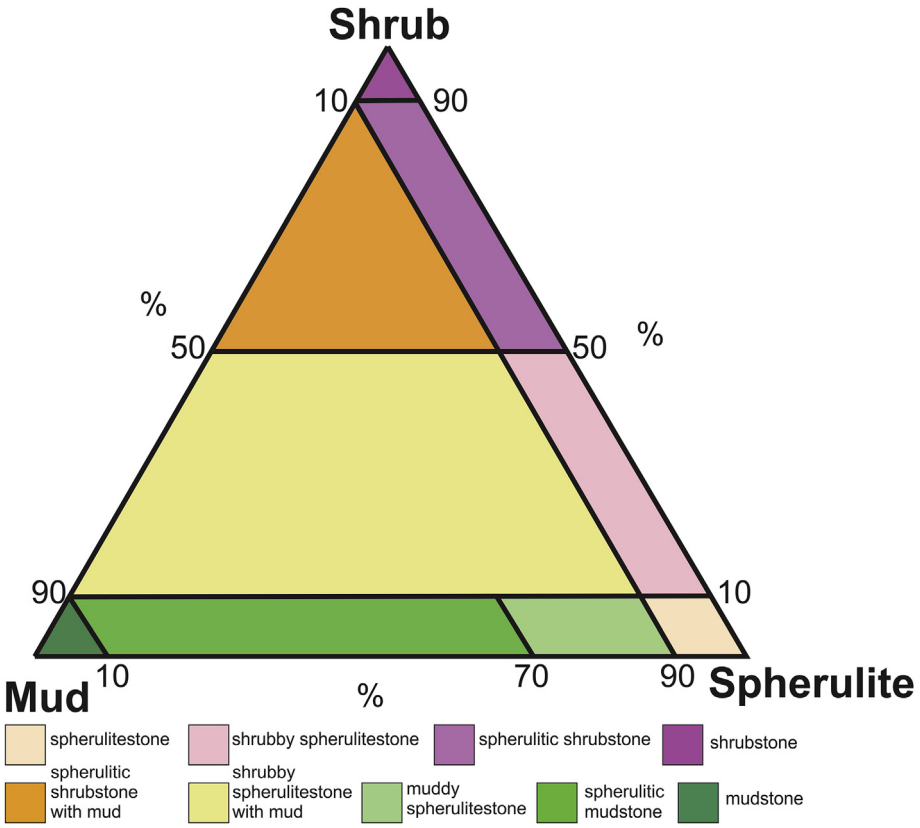

Fig. 8. Ternary diagram showing the facies classification for sediment generated *in situ* for the Barra Velha Formation.

porosity and permeability measurements to provide a better understanding of reservoir characteristics and trends.

5. Application of facies classification to the Barra Velha formation

5.1. Thin-section scale application

Fig. 11 shows an application of the proposed facies classification to the study area (Fig. 1C), based on descriptions of 1921 thin-sections. Estimated proportions of different components were plotted for each sample on the ternary diagrams, differentiating data from the wells drilled on the palaeo-high and those located on the eastern side of the structure towards the deeper basin. Samples with > 90% mud are plotted on ternary diagrams for both the in-situ and reworked facies (A1 and C1) as it is not possible to unambiguously determine their origin, and they are further discriminated in the mudstone ternary diagram (B1).

The *in-situ* facies (Fig. 11 A1 to A3) show a higher proportion of Mg-clay in the deeper wells, whereas wells drilled on the palaeo-high show a predominance of facies composed of spherulites and shrubs. For all samples with < 90% spherulite + shrubs and < 90% mud, the fine-grain fraction is exclusively comprised of Mg-clay. In contrast, the triangle for mudstone (Fig. 11 B1 to B3) shows that most samples with > 90% mud are composed of varying proportions of calcite and dolomite, with < 5% of mudstone samples containing > 10% Mg-clay minerals. The triangle for reworked facies (Fig. 11 C1 to C3) shows a higher abundance of grainstone/rudstone in samples from the wells drilled on the palaeo-high and of mudstone/wackestone/packstone from those drilled more basinward. Reworked facies are bimodal, tending towards either grain-supported (> 75% coarse grained) or mudstone, with a relative paucity of packstone (Fig. 11 C).

5.2. Metre-scale application

The methodology proposed by Muniz and Bosence (2015) was applied to interpret the facies in the 8 wells as described above in the Materials and Methods section. Fig. 12 shows that there are differences in the distribution of facies between the upper and lower portion of the Barra Velha Formation, as well as between the wells drilled upon the palaeo-high and more basinward on the structure. The basal portion of Lower Barra Velha Formation is largely composed of Mg-clay-, calci- and dolo-mudstone, and reworked facies, whereas the overlying portion is mostly formed by *in situ* facies with or without Mg-clay minerals. There is a marked increase in Mg-clay facies above the Intra Alagoas Unconformity. In the wells drilled off the main structure, Mg-clay minerals predominate, but decrease in abundance towards the top of the Upper Barra Velha Formation where *in-situ* facies lack Mg-clay minerals. The wells drilled upon the palaeo-high are composed of mudstone and reworked facies above the Intra Alagoas Unconformity, giving way upwards to a dominance of *in-situ* facies up to the Salt Base Unconformity, showing rare (less than 0.1%) facies with Mg-clay. Facies in the uppermost 15 m of the Upper Barra Velha Formation in all eight wells are distinct, with an increase of mudstone but a lack of Mg-clay minerals, and evidence of microbial textures (“Lula's Fingers”). Elsewhere, in an adjacent field within the Santos Basin, Artagão (2018) interpreted this interval as postdating the basal unconformity, representing the lowermost part of the Ariri Formation. However, Tedeschi (2017) has shown an important change on strontium isotope values ($^{87}Sr/^{86}Sr$ ratios) at limit between the top of “Lula's Fingers” (ˆ0.712) and the base of the anhydride (~0.709) in a cored section from Santos Basin. Therefore, it is likely that the main uniformity is at the base of the anhydride layer above the “Lula's Fingers”.

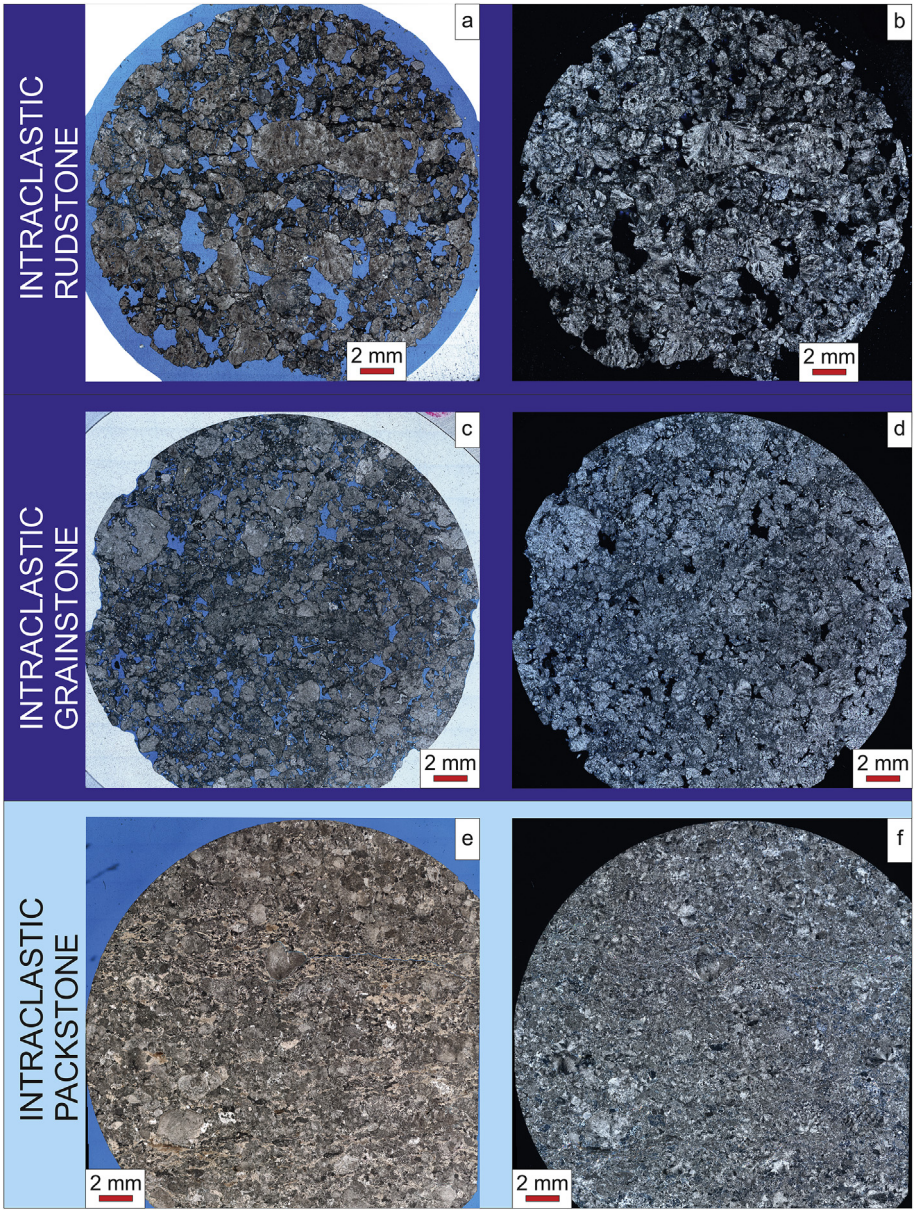

Fig. 9. Classification for reworked facies: a) and b) intraclastic rudstone with inter-particle porosity; c) and d) intraclastic grainstone with inter-particle porosity; e) and f) intraclastic packstone. All image pairs are PPL and XP.

5.3. Bulk chemical data and detrital grain distribution

Chemical analyses were undertaken to determine the extent to which the various proposed facies types can be distinguished on the basis of their chemical composition, and to identify any chemical variations within and between these facies (Fig. 13). As an example, Fig. 14a shows the bulk chemical distribution of Al_2O_3, Fe_2O_3, TiO_2, and K_2O relative to the proposed facies classification. In general, all samples have a low iron content (< 1.2%), but facies rich in Mg-clay have higher values when compared with mud-poor facies. Apart from the mud-poor facies, all facies have a similar mean value. However, the spherulitestone has the highest content of Fe_2O_3, but they are outliers values. Al_2O_3, TiO_2 and K_2O follow a similar interpretation regarding value abundance within facies.

Detrital minerals (Fig. 15) are present within the carbonate facies but their abundance is relatively low (in general < 7%). Most detrital minerals are silt to fine sand-size grains, and are comprised of K-feldspar, albite, quartz and mica. These detrital minerals can be incorporated within spherulites, shrubs and mud and they occur in pore spaces. Considering the K-feldspar content as representative of detrital grain abundance, of all the proposed facies types those rich in mud have significantly higher median detrital content (Fig. 15b). Most facies with a low mud content have a low median detrital content, but the subset of these samples with > 0.5 vol% detrital grains (marked as outliers in Fig. 14b) suggests that the detrital content increases with abundance of spherulites.

Principal Component Analysis (PCA) was applied to interpret the geochemical and XRD data (Wold et al., 1987) and estimate the correlation structure of the variables (Fig. 16a), using the eigenvalues to evaluate the variation represented by each principal component (Fig. 16b). There is a clear correlation between detrital grain abundance and the majority of trace elements at component 1 (Al_2O_3, Fe_2O_3, TiO_2, and K_2O). Al, Fe and Ti are generally considered as elements that have a low mobility during weathering, transport and diagenesis (Sugisaki et al., 1982; Yamamoto et al., 1986; Wintsch and Kvale, 1994). This relationship therefore suggests that the detrital grains are a source of these chemical components. There are three additional components that exhibit a different behaviour. Component 2 is composed of MnO,

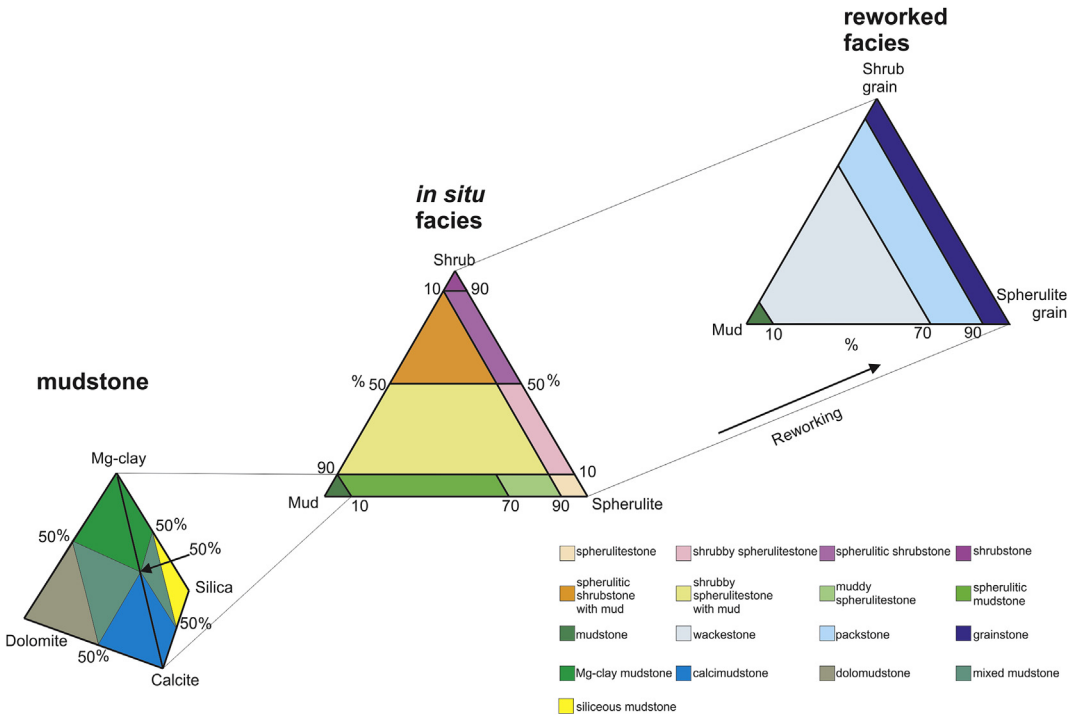

Fig. 10. New classification scheme, comprising three triangular diagrams, proposed to describe all facies within the Barra Velha Formation.

NaO, P_2O_5 and CaO; SiO_2 forms component 3 (unusually in this case Si appears to be independent of Al, suggesting that silica and Mg-clay minerals have other sources than detrital, which agrees with authigenic source in alkaline lakes), and the 4th component is composed of MgO and Cr_2O_3, in which this relationship is not common. However, the amount of Cr is close to the detection limit, which could induce to false correlation with other elements.

6. Discussion of the origin of the main facies components

Mud: The main clay minerals present in the Barra Velha Formation are Al-free Mg-silicate minerals (Tosca and Wright, 2015), formed and preserved in the sub-littoral zones. They do not occur in organic-rich profundal intervals, however, where Mg-clays would dissolve. Dissolution of the clays would have led to the release of significant amounts of sodium, silicon and magnesium into the lake or pore-water.

The occurrence of syngenetic Mg-clay minerals in alkaline and saline lacustrine environments is well documented (Millot, 1970; Darragi and Tardy, 1987; Calvo et al., 1999). From laboratory experiments, the kinetic boundary for the precipitation of Mg-clay minerals in the absence of any bacterial influence has been determined (Tosca and Wright, 2015; Tutolo and Tosca, 2018). The identification of Mg-clay minerals in association with biofilms and microbial carbonate (Bontognali et al., 2010; Perri et al., 2018) suggests that microbial activity could catalyze the precipitation of these minerals. Tosca and Wright (2015) suggested that biotic processes would depend more on the local bacterial distribution within the substrate where the clay minerals would have nucleated such that the Mg-clay distribution would be more heterogeneous. However, bacteria may be widely distributed in such environments and thus laterally extensive accumulations of Mg-clay minerals would be the likely product of both biotically-mediated precipitation and of precipitation driven by abiotic process, such as evaporation. Considering the discussion above, the presence of Mg-clay minerals suggests a low-energy, alkaline lacustrine environment; higher-energy conditions would likely prevent clay deposition, removing them to quieter areas. In addition, preserved Mg-clay facies indicate little change in pore-water chemistry, otherwise the minerals would have been dissolved.

Laminated fine-grained muddy facies are suggested by Lima and De Ros (2019) to have been originally deposited as laminated clays, probably stevensite, and to have been extensively replaced by calcite, dolomite or quartz. They identified relics of the precursor clays, as well as organic matter and siliciclastic grains (quartz, biotite and muscovite). Indeed, in some thin-sections, microcrystalline dolomite has clearly replaced Mg-clay minerals (Lima and De Ros, 2019), but in others, there is no evidence for this. In some thin-sections, microcrystalline calcite and microcrystalline dolomite occur together, suggesting replacement of calcite by dolomite. Dolomite is likely to have been precipitated via a metastable precursor. Microcrystalline calcite could be formed either within the depositional environment and/or during very early diagenesis.

Some authors (Sartorato, 2018; Artagão, 2018; Farias et al., 2019) interpreted these deposits as only forming during flood events, with an input of terrigenous siliciclastic material and dolomite crystals precipitated at the air-water and/or chemocline interface (Farias et al., 2019); it has been suggested they formed within extracellular polymeric substances (EPS) (Sartorato, 2018; Artagão, 2018). Anyway, the presence of dolomite indicates the presence of Mg in the system, which could be derived from the EPS ($Mg2+$ ions being attracted there) or derived from the Mg-clays. Although we cannot define which process is operating, it is important to consider microcrystalline dolomite in the classification of the Pre-salt rocks.

Microcrystalline silica (Fig. 5) is also a matter of discussion. In the study area it does not occur within microbial boundstone as described by Saller et al. (2016) nor are there any hydrothermal silica deposits, as described in the Pão de Açúcar area of the Campos Basin (Viera de Luca et al., 2017) similar to those in Lake Bogoria (Kenya Rift Valley; Renaut and Tiercelin, 1994). However, silica nodules and layers alternating with mudstone are common. The silica could be derived from dissolution of Mg-clay minerals (Lima and De Ros, 2019; Wright and Barnett, 2019), resulting from a change in pore-water chemistry. There is also the possibility of silica derived from diatoms (e. g., Renaut and Tiercelin, 1994), but we have not found any evidence for this. Nevertheless, microcrystalline silica is an important fine-grained material

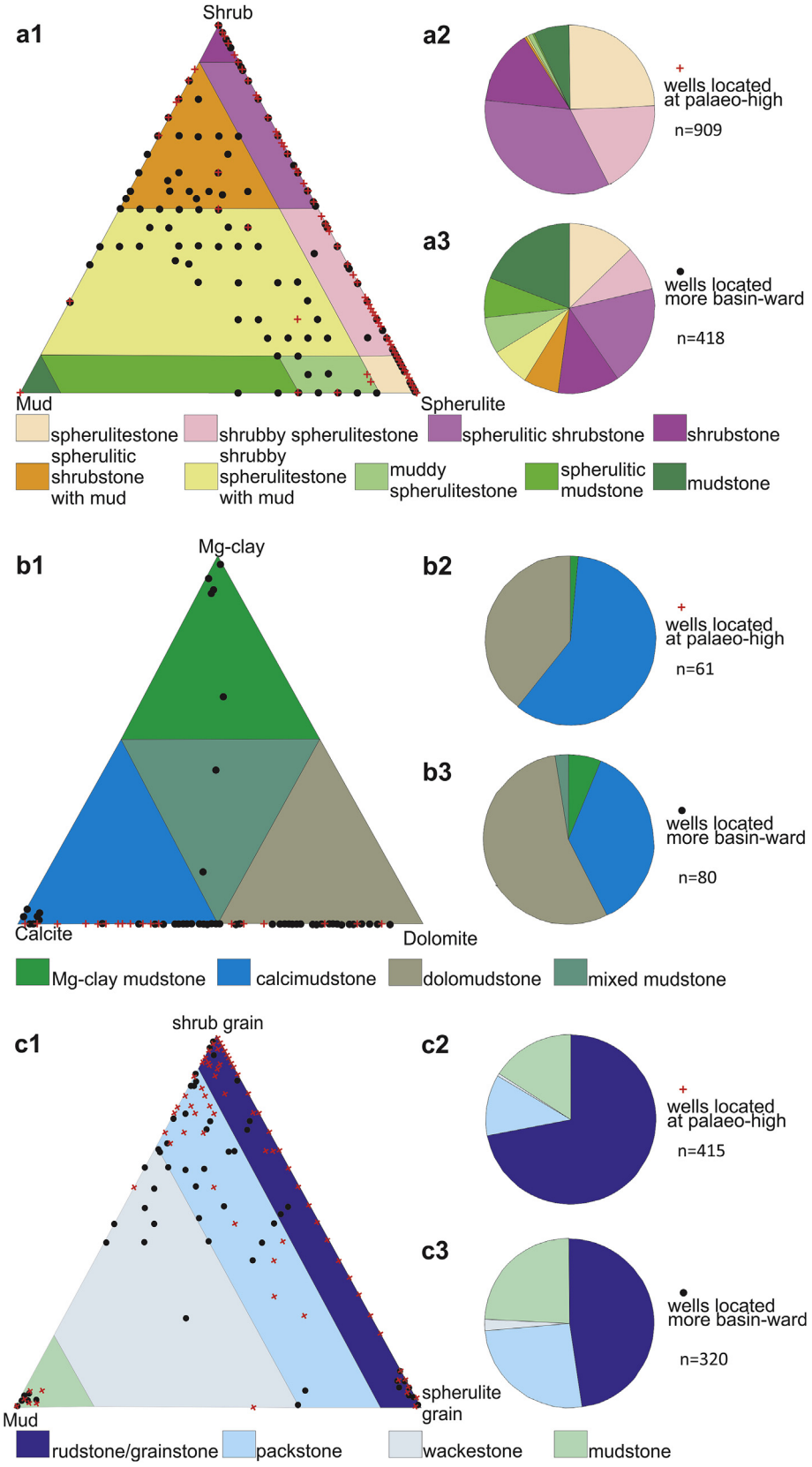

Fig. 11. Application of the facies classification to 8 wells in the Barra Velha Formation for the study area shown in Fig. 1C, differentiating wells drilled on the palaeo-high (red crosses) and more basinward (black circles). Ternary diagrams and pie charts show the distribution of in-situ facies (A), mudstone components (B) and reworked facies (C). (For interpretation of the references to colour in this figure legend, the reader is referred to the Web version of this article.)

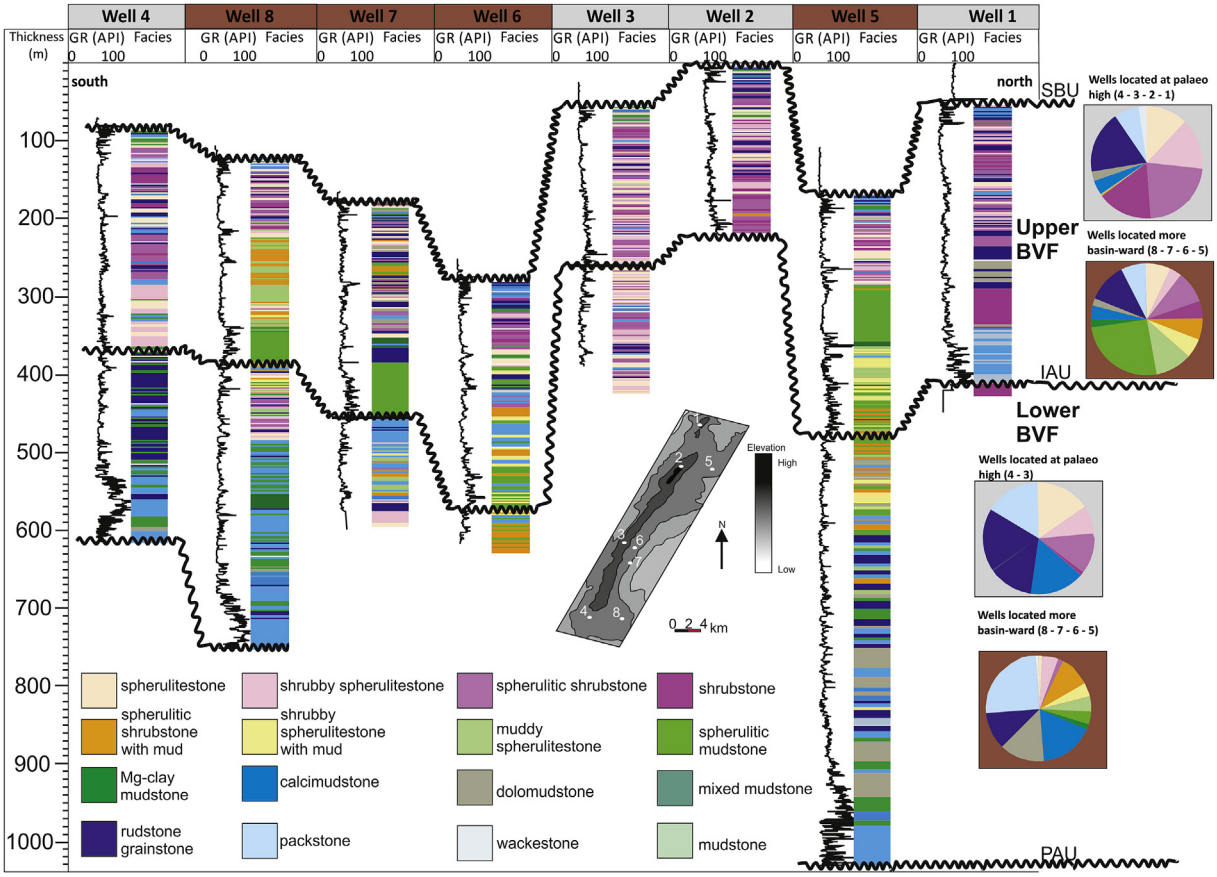

Fig. 12. Cross-section showing facies distribution for the 8 wells and the three main unconformities within the Barra Velha Formation. The distribution of facies shows a predominance of Mg-clay at wells drilled more basin-ward, whereas in-situ carbonate facies occur in the wells drilled on the palaeo-high. BVF = Barra Velha Formation, PAU = Pre-Alagoas Unconformity, IAU = Intra-Alagoas Unconformity, SBU = Salt Base Unconformity.

that potentially could provide information on changes in lake-water chemistry and/or pore-water during diagenesis. Thus, in a pragmatic approach, we identify four types of mud: Mg-clays, microcrystalline calcite, microcrystalline dolomite and microcrystalline silica. Their proportions as seen today are important in the classification of Pre-salt rocks and for the interpretation of pH and other environmental and/or diagenetic conditions that prevailed during formation of the Barra Velha facies.

Spherulites: The majority of spherulites within our study occur within deformed Mg-clay-rich and calcitic mudstone, displacing the fine material, suggesting that the spherulites grew while the sediments were unconsolidated in a very early stage of burial. Such petrographic evidence has been interpreted to indicate that these spherulites formed within a matrix, either replacively (Herlinger et al., 2017; Souza et al., 2018; Lima and De Ros, 2019) or displacively (Wright and Barnett, 2015, 2019), in the very shallow subsurface below the water-sediment interface.

However, 35% of the 271 spherulitestone samples examinated show interpenetration of spherulites on compaction and an absence of inter-spherulite sediment. These features strongly support the interpretation that the cortical crystals did not grow displacively within sediment, but grew at the sediment-water interface (Chafetz et al., 2018). This could indicate that at least some of the Barra Velha Formation spherulites nucleated around clumps of bacteria in the water column and then settled to the bottom for continued cortical crystal growth. The spherulites may have rolled around at the sediment-water interface and grown incrementally via a mechanism similar to that proposed for other calcitic spherulites grown in alkaline lakes (Mercedes-Martín et al., 2017). If currents were strong, then any clay would likely have been removed from the site of spherulite precipitation. 65% of spherulitestone samples examined were formed *in situ* in the subsurface. 35% could have formed either *in situ* in the water column, at the lake-bed or in the subsurface and may have been reworked later. Whilst the proposed new classification allows a grainstone (reworked facies) to be exclusively compose of spherulitic grains, in practice there is limited thin-section evidence allowing differentiation between such a reworked spherulitic grainstone and a spherulitestone that formed *in-situ*.

Alternatively, spherulites that show interpenetration on compaction and an absence of inter-spherulite sediment could also be early diagenetic and formed within Mg-clay or microcrystalline calcite. However, if currents were strong, then any fine-grained components would have been removed from the site of spherulite precipitation by either hydrodynamic selection or dissolution of these components. In both cases that spherulites show interpenetration on compaction and an absence of inter-spherulite sediment, we suggest that they are referred as grains. Resulted from been formed on the interface sediment-water or been a product of hydrodynamic or chemical selection, they would be a grain (Dunham, 1962).

In the course of their laboratory experiments, Mercedes-Martín et al. (2016) discovered that spherulites were more likely to have formed extensively at the sediment-water interface in alkaline lakes that were rich in dissolved organic acids, suggesting that clay-gels were not required to form voluminous deposits of spherulitic grains. Rogerson et al. (2017) and Mercedes-Martín et al. (2017), examining deposits from the Lower Carboniferous East Kirkton Limestone, Scotland, demonstrated that the formation of spherulitic carbonates could be decoupled from the abundance of clay in alkaline lakes and concluded that 'microbial-solution' interactions warrant further research. Indeed, Kirkham and Tucker (2018) suggested that permineralised bacteria (or viruses), within the water or within the sediment, could provide the

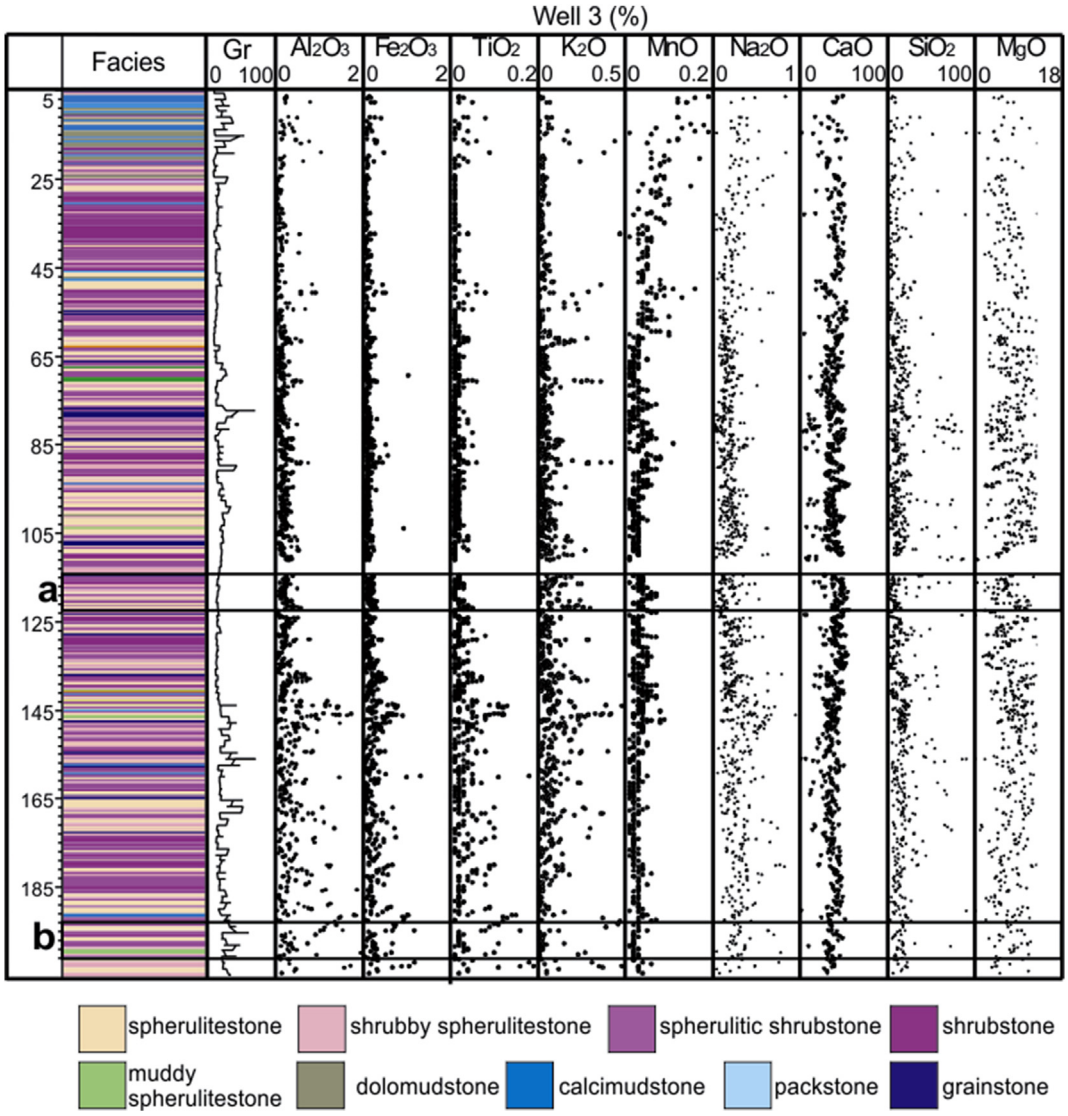

Fig. 13. Distribution of elemental geochemistry. Box a and b are detailed in Figs. 14 and 19.

nuclei for spherulite growth, meaning that spherulite formation was initiated by microbial activity, but that the crystal growth itself is abiotic.

Shrubs: Shrubs are interpreted in this study to have formed by *in-situ* growth upward from a substrate, suggesting a higher rate of precipitation at sites near the top of the shrubby layer where the advective supply of reactive ions is greater than closer to the substrate. Terra et al. (2010) suggested adopting the term stromatolite (*sensu* Riding, 2000). They described laminated deposits comprising layers of individual shrubs which branch as they grow upwards, forming convex structures. However, many authors (Wright and Barnett, 2015; Herlinger et al., 2017; Souza et al., 2018; Lima and De Ros, 2019; Farias et al., 2019) described these deposits as some type of abiotic carbonate with morphometric similarities suggesting controlling processes comparable to those in travertine systems. These authors, however, noted the lack of features typical of travertine, such as cascades, pisoids, flow carbonates, vents and gas-bubble spheres (Farias et al., 2019). Our observations accord with those of previous studies suggesting rapid precipitation from highly saturated solutions (Wright and Barnett, 2015), changes in the lake water chemistry related to climate, abiotic precipitation related to CO2 loss by evaporation, magmatic CO2 input and hydrothermal activity (Lima and De Ros, 2019). This would thus support the conclusion that the use of the term stromatolite is inappropriate.

The question of the role of biological factors in the initiation of calcite shrub precipitation or even to facilitate carbonate nucleation remains open. Ceraldi and Green (2017) suggested that shrubs are a microbial-influenced facies and may represent shallow-water deposition affected by wave base and, potentially, also the depth of the photic zone. This interpretation is supported by observations in the Kwanza basin (Saller et al., 2016), where the shrubs are interpreted to form positive topographic structures, similar to biotic reefs, in which growth is oriented towards the light.

Alternatively, Farias et al. (2019) proposed a depositional model for the Barra Velha Formation, invoking similar processes to those in an evaporative basin based on criteria used by Lowenstein and Hardie (1985) in modern salt pans. The proposed model proposes an alternation of periods of flooding, which transforms the salt pan temporarily into a brackish lake, and subsequent periods when the basin is solely groundwater-fed and evaporative concentration leads to desiccation. The alternating layers of shrub, spherulite and mud in the BVF are proposed by Farias et al. (2019) to be the equivalent of alternating halite and mud layers that characterize salt pan deposits. The shrubs are thus interpreted to have been generated at the sediment-water interface during evaporative periods, implying that shrub formation reflects climatically-control lake-level oscillations. Calcitic spherulites are interpreted to form diagenetically within a Mg-clay below the saline pans.

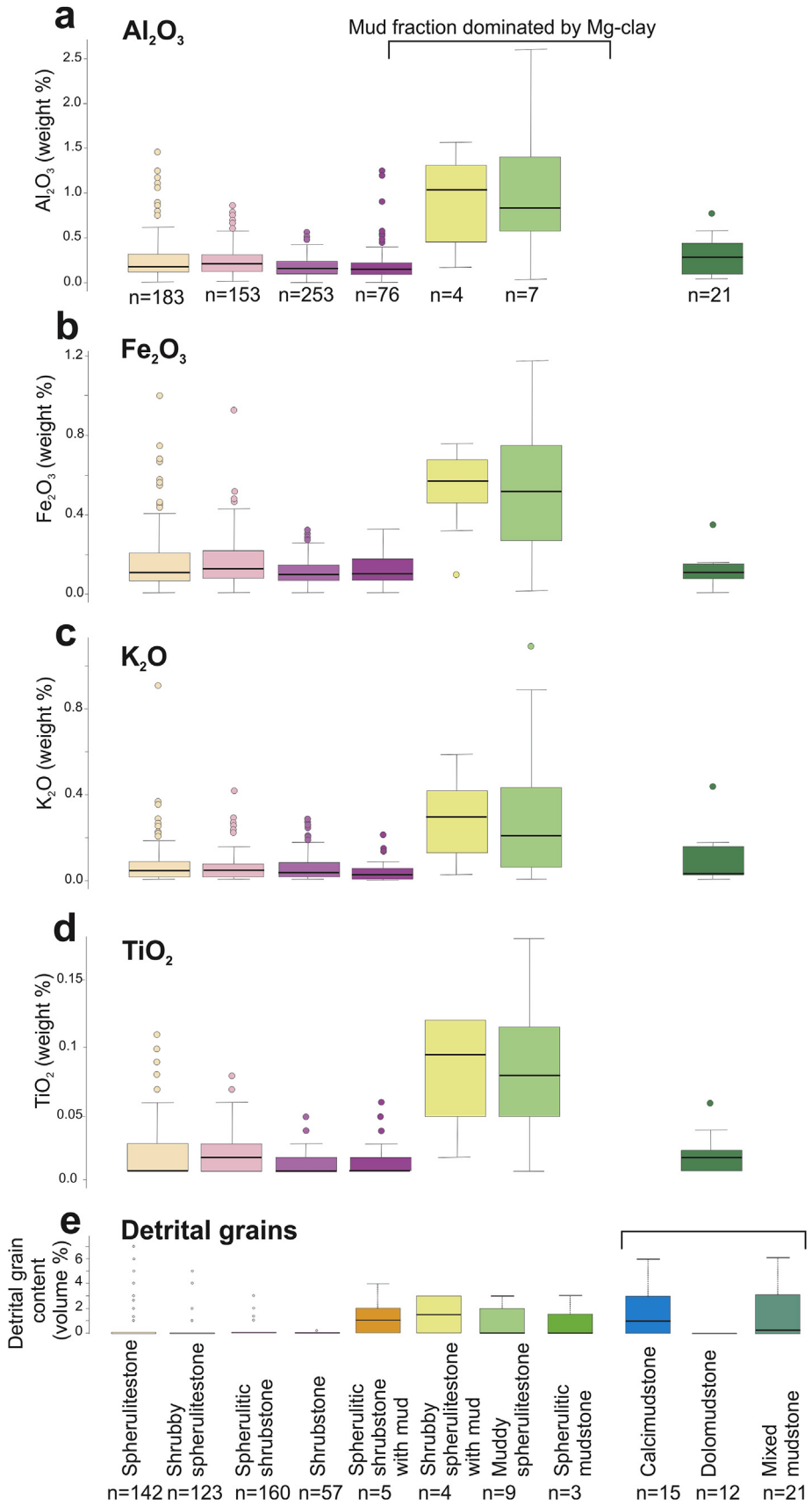

Fig. 14. a) Boxplots showing the distribution of a) Al2O3, b) Fe2O3,c) K2O and d) TiO2 within the described facies based on ICP analysis for samples from Well 3. e) Boxplots showing the distribution of K-feldspar within the described facies based on XRD analysis for all wells. n = number of samples.

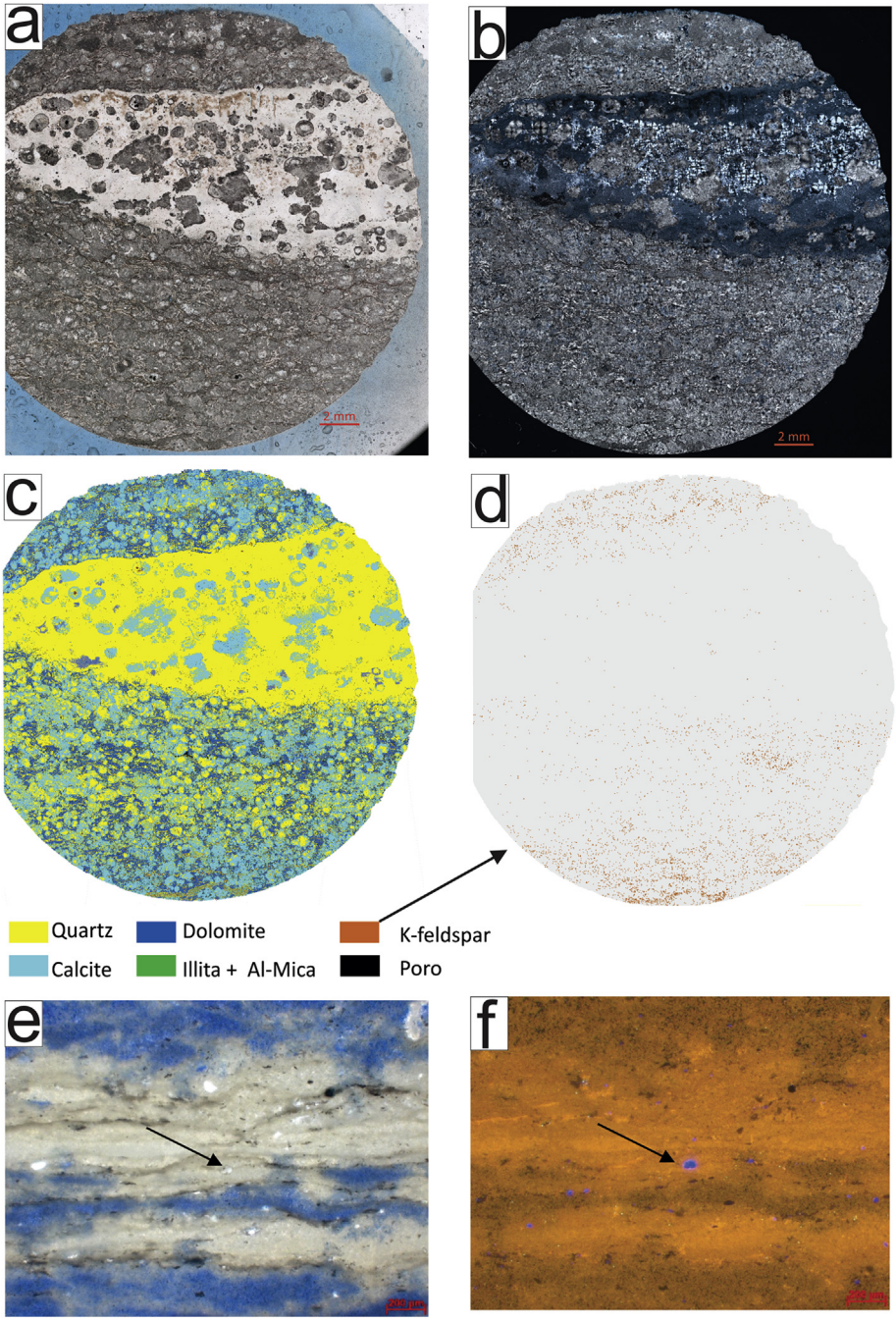

Fig. 15. a) and b) spherulitestone cemented by dolomite, chalcedonic and micro-quartz. Image pairs are PPL and XP. c) QEMSCAN mineralogical map of all components and d) showing distribution of K-feldspar. e) petrographic image and f) cathodoluminescence image of mudstone, with black arrow pointing to K-feldspar.

7. Facies patterns and the ideal cycle in the Barra Velha formation

Prior to our proposed scheme there has been no generally accepted system of nomenclature to describe the complete range of facies and proportions of shrubs, spherulites and mud which form the Pre-salt carbonate rocks. Many published articles (e.g. Wright and Barnett, 2015; Muniz and Bosence, 2015; Wright and Barnett, 2017; Liechoscki de Paula Faria et al., 2017; Arienti et al., 2018; Artagão, 2018; Sartorato, 2018; Farias et al., 2019; Tanaka et al., 2018; Lima and De Ros, 2019) have simplified this complexity by choosing end-member components to name the facies, ignoring the gradation from one end-member to another. However, in the section discussing the origin of the main facies components it is shown that different processes could be responsible for forming each component. Adding the abundance of each component in the name facilitates the understanding of depositional and diagenetic environmental changes through time by considering the intermediate scenarios. This also allows for more detailed studies of cyclicity and depositional facies models.

7.1. Scale-dependency of facies distribution

The three main components, shrubs, spherulites and mud-size grains, may alternate in their occurrence on a cm scale in thin-sections (Fig. 6 c to f) or at a macro-scale in core (Fig. 17). To deal with this heterogeneity, the approach discussed by Liu et al. (2002) suggested interpreting at different scales for different purposes. Meso-scale

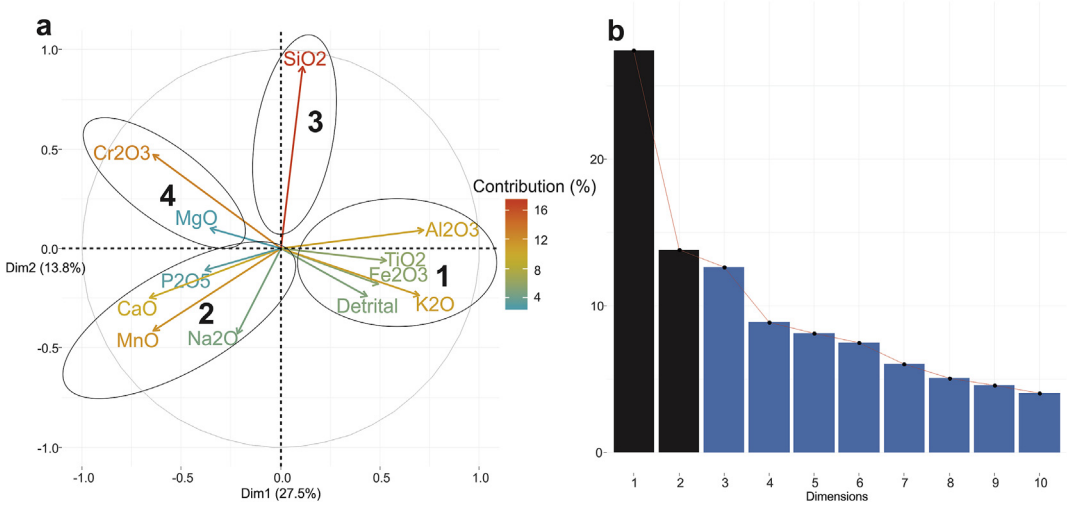

Fig. 16. a) Correlation circle map showing results from the most significant two dimensions identified by the PCA analysis (which together represent 41.3% of the total variance), where the most highly correlated variables group together. Each component (1, 2, 3 and 4) follows a different pattern. b) Scree plot showing the Eigenvalues (quantification of variance) according to the dimensions analyzed. In black the two dimensions plotted at a.

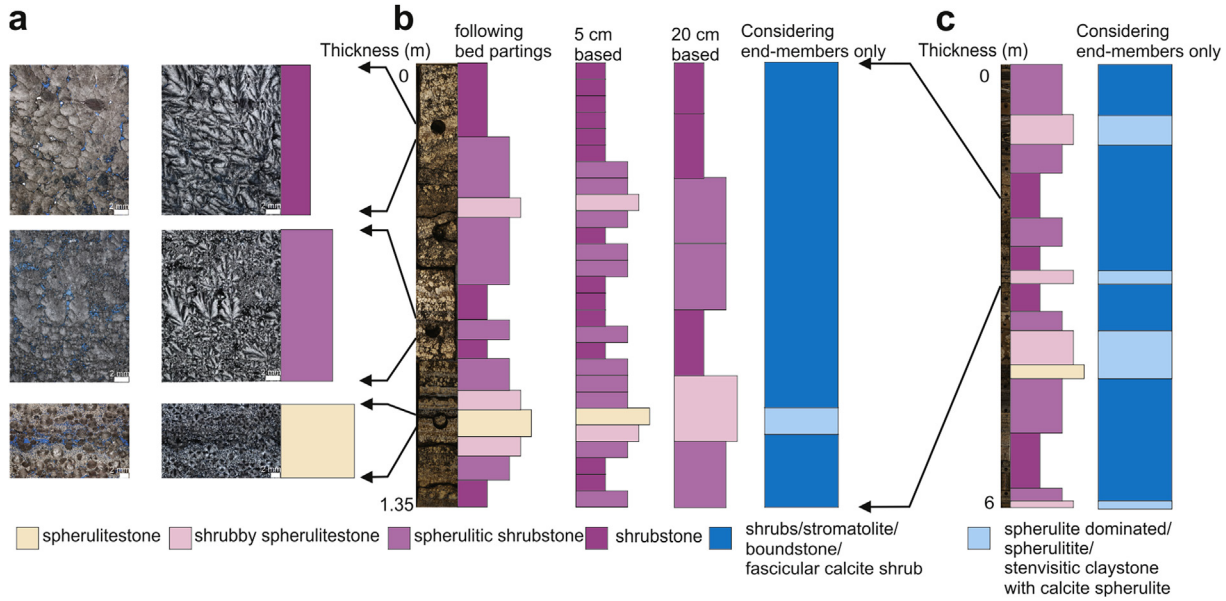

Fig. 17. a) Representative examples of facies at thin-section scale. b) Core facies description with different examples of upscaling. c) Facies up-scaled for elementary sequence scale. Names stromatolite and spherulite (Terra et al., 2010), fascicular calcite shrub and stevensite claystone with calcite spherulite (Herlinger et al., 2017; Lima and De Ros, 2019), shrubs and spherulites (Farias et al., 2019) and boundstone (Sartorato, 2018).

(10–100's mm) facies logging would be used for understanding the depositional and diagenetic processes, as discussed earlier in this article, whereas macro-scale (1–10's m) facies logging serves the purposes of analysis of facies and architectural elements. Mega-scale (10's m) facies logging would be used for identification of major reservoir units and for correlation between outcrops and wells, and also for interpreting major changes in the depositional system. The proposed facies classification is a powerful tool to transform the meso-scale occurrence of components to a higher-resolution scale with a minimum of information loss by recalculating the proportion of which components occur on the desired scale.

The new facies classification allows an analysis of the vertical facies variation and horizontal correlation across the field with minimal loss of depositional and diagenetic information. Fig. 17a shows an example of heterogeneity at the meso scale (mm-cm) and presents different possibilities to upscale (Fig. 17b) to the macro-scale whilst preserving the identified heterogeneity. Units defined from bed partings observed in core are compared with those derived from uniform spaced intervals (5 and 20 cm in Fig. 16), and can be used to suggest an appropriate thickness to be considered for an unsupervised scheme. This classification scheme also recognizes systematic changes in the vertical distribution of facies classes that can be used as a basis for analysis of cyclicity. In contrast, a facies classification scheme that considers only the end-member components results in a sequence dominated almost exclusively by shrubs, which may be appropriate at the macro to mega scale but fails to adequately describe important variations at the scale of the elementary sequence.

7.2. Facies stacking patterns within a basic cycle

The stacking of facies commonly reveals a hierarchical pattern with the highest frequency-cycle being the basic cycle or elementary sequence *sensu* Strasser et al. (1999), where facies repetition corresponds to the shortest recognizable rhythm of environmental change with a

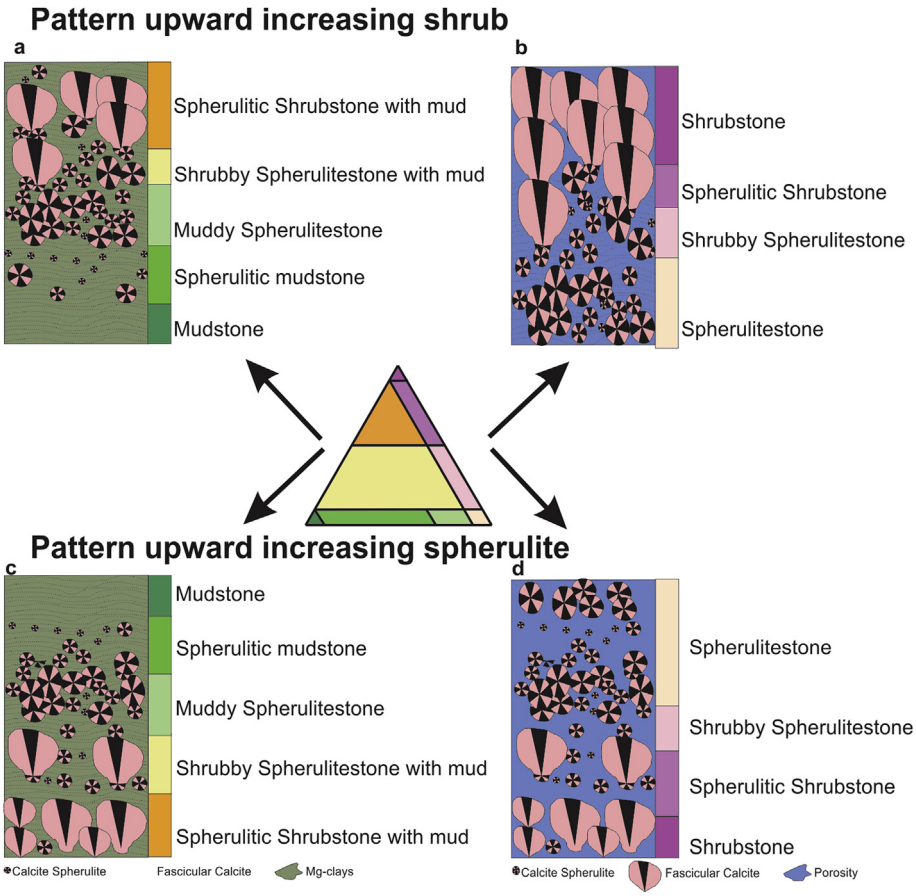

Fig. 18. Two models (upward-increasing shrub and upward-increasing spherulite) of facies stacking for elementary cycles in the Barra Velha Formation based on core descriptions and two types of cycle. a) and c) non-reservoir and b) and d) reservoir.

regional significance. Such basic cycles generally consist of one bed, or rarely two, as has been described in marine systems where both the sequence boundary and the maximum-flooding surface/interval are highlighted by increased abundance of clays (Pittet and Strasser, 1998). However, there has been much discussion over the presence of hierarchical patterns in sedimentary sequences (Pollitt et al., 2014).

Within the lacustrine system, cycles can be identified in both reservoir intervals that are mud-poor, and also in more mud-rich non-reservoir intervals, which have more than 10% clay and thus little porosity. In both types of interval, two possible patterns for facies stacking of the basic cycle can be suggested after upscaling to the macro-scale (Fig. 18). Several models for a basic cycle have already been proposed for the Barra Velha Formation and its equivalent in the Campos Basin (Wright and Barnett, 2015; Muniz and Bosence, 2015; Liechoscki de Paula Faria et al., 2017; Arienti et al., 2018; Artagão, 2018; Sartorato, 2018; Farias et al., 2019; Lima and De Ros, 2019). These researchers all suggest a dominance of shrubs within the upper part of the basic cycle (Fig. 17 a and b). This facies stacking pattern (here termed Upward-increasing shrub pattern) is composed in non-reservoir intervals of an upward transition from mudstone, to spherulitic mudstone, muddy spherulitestone, shrubby spherulitestone with mud and lastly to spherulitic shrubstone with mud. Where the abundance of mud is < 10% (within reservoir intervals) the stacking pattern within a basic cycle generally consists of an increasing upward abundance of shrubs, from spherulitestone to shrubby spherulitestone, spherulitic shrubstone and finally to shrubstone. A key feature of the Upward-increasing shrub pattern is the irregular surface above the shrubstone, which represents the top of this ideal cycle and may or may not have been subaerially exposed. An alternative facies stacking pattern (here termed the Upward-increasing spherulite pattern) would be shrub dominated at the base, with a gradual transition upward to spherulitestone and, in non-reservoir intervals, also mudstone (Fig. 18 c and d). In this analysis the reworked facies, comprising < 20% of the samples have not been included in the idealized basic cycles for *in-situ* sediment (Fig. 19), but they could be added to the cycles according to their occurrences.

Supplementary data for Al_2O_3, Fe_2O_3, TiO_2 and K_2O from the whole-rock chemical analysis were used to help characterize the basic cycles within the Barra Velha Formation in the study area. The vertical distribution of detrital grains (Figs. 14b and 15) within an 8-m length of section representative of the Upper Barra Velha Formation is shown in Fig. 19. Within the basic cycles a higher proportion of detrital grains occurs in the mud-rich facies, as well as in the spherulite-rich facies. Using this compositional data for Well 3 (the most complete record from core), and the direct association with facies stacking patterns, we characterize the thickness of basic cycles for all 6 cored wells in the study area. This analysis suggests a mean thickness of the basic cycle in the region of the palaeo-high of 1.6 ± 0.8 m, (n = 200), with a range from 0.3 to 4.8 m. In comparison, basic cycles from wells located more basin-ward, have a mean of 2.0 ± 1.3 m (n = 35) and a range from 0.6 to 7.6 m. In addition, the cycles in these deeper wells are more mud-rich, whereas the mud-poor type of cycle is more common in the upper part of the palaeo-high succession (the reservoir interval).

7.3. Process-based models for the basic cycle

The two alternative facies stacking patterns (a and b - Fig. 18) suggested for a basic cycle within both reservoir and non-reservoir intervals can be interpreted using concepts derived from a traditional sequence stratigraphic approach for marine carbonate sediments based

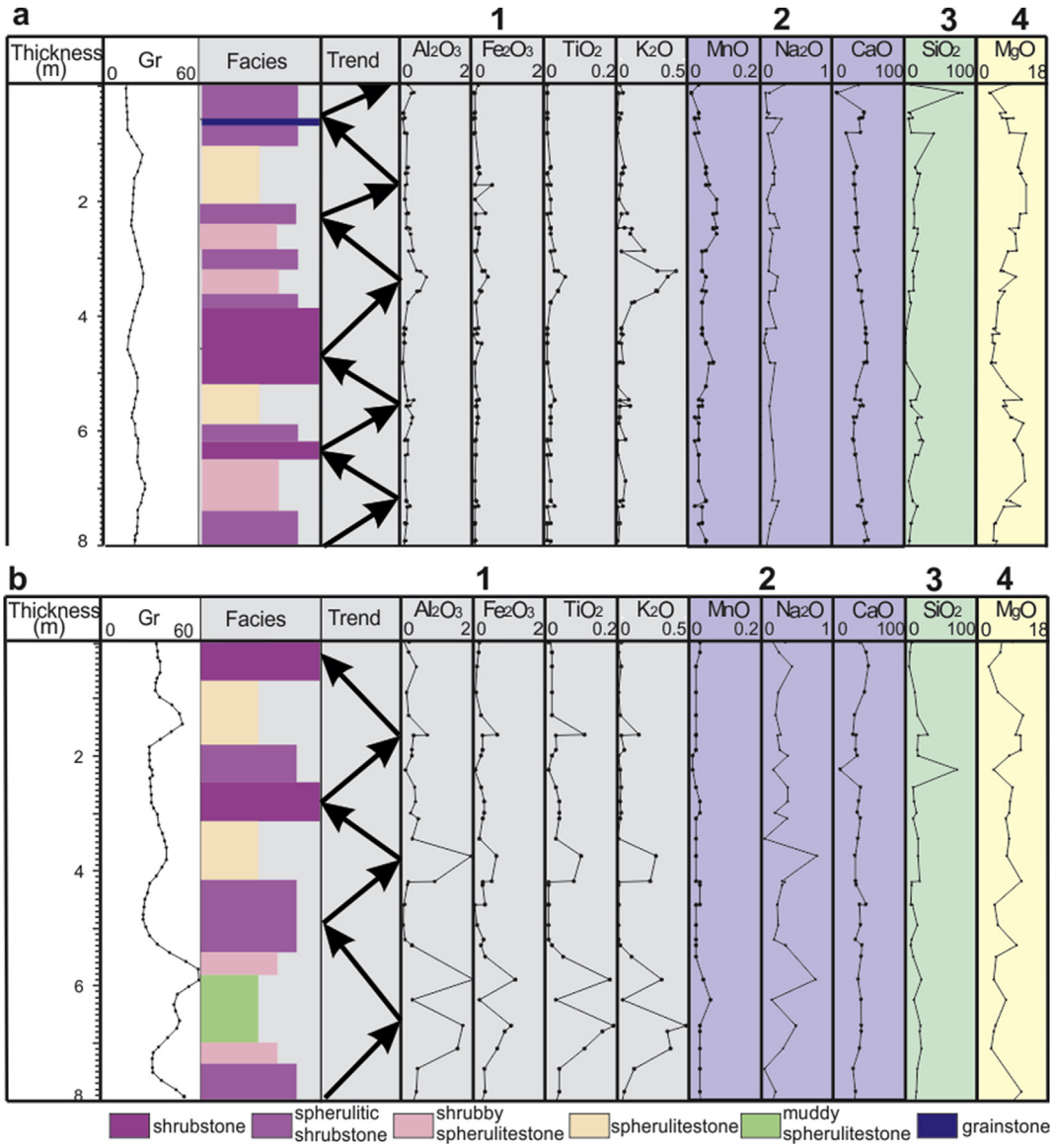

Fig. 19. Vertical distribution of major chemical components within the proposed facies classification for two 8 m thick intervals shown in a) and b). PCA showed the association between increasing abundance of detrital grains, Al, Ti, Fe and K within spherulitestones. 1, 2, 3 and 4 are components following a different pattern.

on changes in water depth. In lacustrine systems changes in facies may be linked to water depth via physical controls such as the depth of wave base, biological controls such as the photic zone depth and/or chemical controls such as evaporative concentration. An alternative interpretation for these BVF lacustrine cycles is that changes in abundance of components are due to temporal variations in lake water chemistry independent of water-depth variations (Mercedes-Martín et al., 2019). In line with this, Garcia-Ruiz (1998) suggested that growth of spherulites is favoured over that of shrubs under conditions of high pH (> 10) and dissolved SiO_2 > 250 ppm. In this case, the facies variation could be interpreted in terms of a less alkaline to more alkaline trend instead of the traditional increase and decrease of accommodation space.

As discussed above, there are a number of models for spherulite genesis. However, irrespective of whether the spherulites formed on the lake surface, or within the water column and then settling and growing on the lake floor or they are a product of early diagenesis within a clay-rich sediment or gel, most authors (Wright and Barnett, 2015; Muniz and Bosence, 2015; Wright and Barnett, 2017; Herlinger et al., 2017; Liechoscki de Paula Faria et al., 2017; Arienti et al., 2018; Artagão, 2018; Sartorato, 2018; Ceraldi and Green (2017); Tanaka et al., 2018; Lima and De Ros, 2019) agree that they most likely formed in deeper water relative to the shrubs (as in the facies stacking pattern of upward-increasing shrub). According to this interpretation, the increase in detrital grain content within the spherulitic and/or mud-rich facies would be associated with fluvial input during wetter periods. The presence of ostracods and fish bones may also reflect the freshening of the basin. In shallower areas of the lake there would likely have been winnowing of mud by wind-waves, and that mud may well have accumulated in the deeper-water areas. Such winnowing may have been more active during periods of higher lake level when the fetch would have increased.

Alternatively, one might expect an increased supply of aeolian material during arid periods to be associated with precipitation of Mg-clay in a more alkaline, shallow lake dominated by evaporation. This would imply that mud was precipitated preferentially during periods of low lake level and this may have provided a substrate within which spherulites could have grown (as in the facies stacking pattern of upward-increasing spherulites). During wetter periods, with an associated reduction in supply of aeolian material, the input of fresh water would

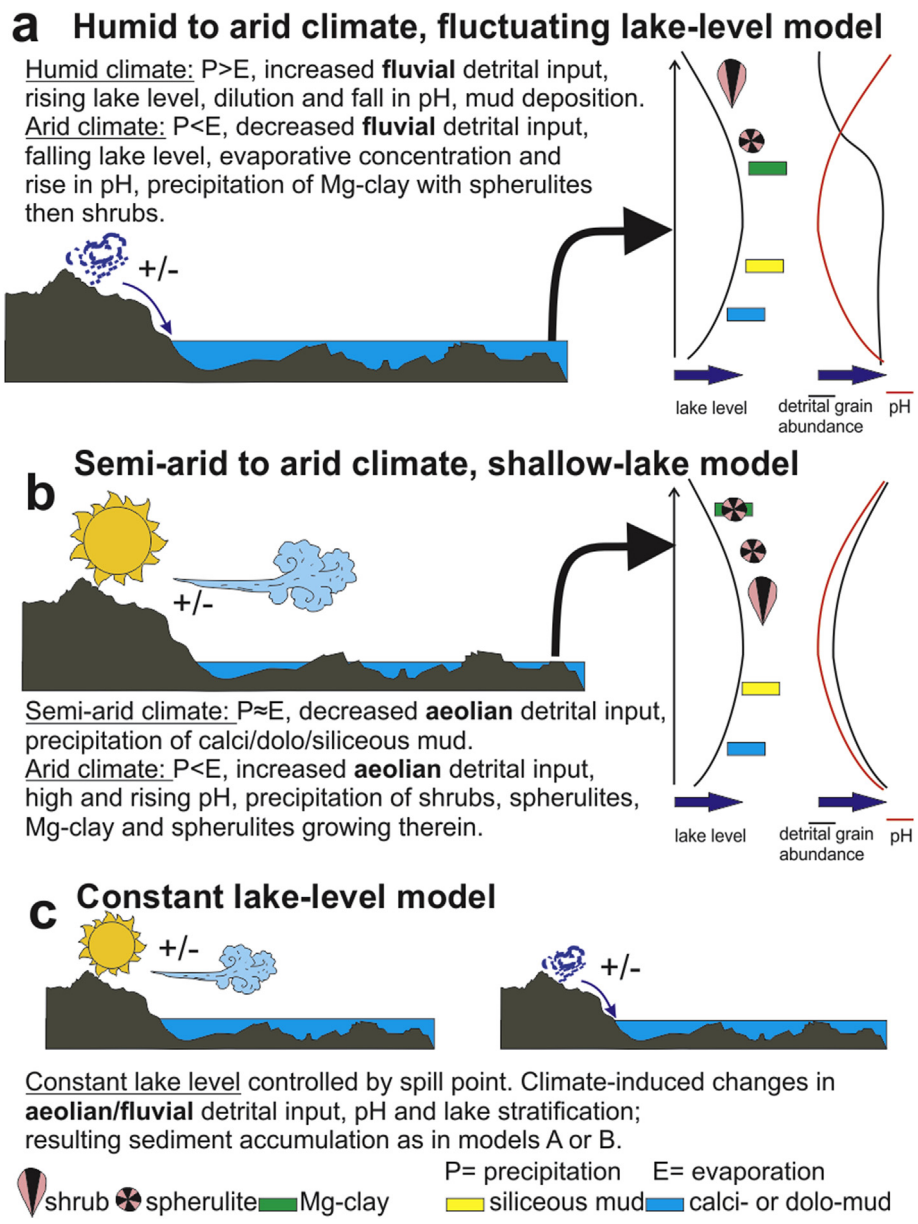

Fig. 20. Alternative conceptual models to explain temporal variations of detrital material within the Barra Velha Formation: a) Humid to arid climate, fluctuating lake-level model. b) Semi-arid to arid climate, shallow-lake model. c) Constant lake level controlled by spill point. Black arrows point at the stage of the model for the lake x-section.

have diluted the lake, decreasing alkalinity. These conditions could have favoured the formation of shrubs during periods of rising/high lake level, though this suggestion remains to be fully explored.

Whilst fluctuation in lake level is one driver for changes in lake water chemistry, a scenario whereby lake level is constant, controlled by a spill-point, should also be considered. This would require the amount of water coming into the lake to be sufficient to maintain the lake level at the spill point. At times of high throughput of water, the detrital input would be elevated, but the short residence time of waters within the lake would limit the development of alkaline conditions. In addition, it is important to consider that many alkaline lakes are stratified, and changes, for instance in fluid throughput, could also drive variation in the depth of the chemocline, with a thicker epilimnion (upper layer) of fresher water during periods of higher detrital input. Finally, alternative drivers for the variation in detrital supply should be considered, for example reflecting tectonically determined geomorphological changes in the catchment, which may be decoupled from lake level. However, it is challenging to envisage a mechanism that could give rise to both high-frequency, repetitive changes in detrital influx and facies variations without invoking a changing climate.

Three possible interpretations are thus suggested (Fig. 20 a, b and c) incorporating not just the main components described but also considering the mechanism by which detrital grains were transported into the basin and the lake chemistry. (1) Humid to arid climate, fluctuating lake-level model. During a humid climate, assuming precipitation is higher than evaporation (P > E), one would expect an increase in fluvial detrital input associated with rising lake level, resulting in lake-water dilution and a fall in pH, leading to mud deposition. During an arid climate, assuming P < E, there would be decrease in fluvial detrital input, associated with falling lake level, resulting in evaporative concentration and a rise in pH, leading to precipitation of Mg-clay with spherulites then shrubs. This interpretation is a modification of the Wright and Barnett (2015, 2017) model, incorporating the distribution of detrital grains. (2) Semi-arid to arid climate, shallow-lake model. Under a semi-arid climate, assuming P ≈ E, there would be decrease of aeolian detrital input (dust) and precipitation of calci/dolo/siliceous

mud. During an arid climate, with P < E and an increase in aeolian detrital input, and rising pH to a high level, one would expect precipitation of shrubs, spherulites, Mg-clay with spherulites growing therein. This interpretation is a modification of the Farias et al. (2019) model. (3) Constant lake level controlled by spill point. In this case, climate-induced changes in aeolian/fluvial detrital input, pH and lake stratification, divorced from changes in lake level, would lead to sediment accumulation as in models a and b of Fig. 20.

Regardless of the mechanism(s) controlling the environment of deposition, in common with other Pre-salt studies, our work suggests that there were particular phases of lake sedimentation during which the shrubs were formed and other phases when spherulites and Mg-clays were precipitated. Our work is novel in that it shows a link between facies and detrital content, at the scale of the basic cycle. Independent of which stacking facies pattern is supported (Figs. 18 and 20), the variation in thickness and facies within each basic cycle can be related to changes in accommodation and/or water chemistry. This raises as to question of whether these basic cycles are organized into larger-scale cycles, or whether they reflect random processes, and to what extent any cycle stacking pattern might contribute to unravelling the process-response system controlling sedimentation in the Pre-salt deposits. Application of the new facies classification scheme to address these questions will be the focus of a subsequent paper.

8. Conclusions

Facies from the Barra Velha Formation in the Santos Basin consist of three main components - calcite spherulites, calcite shrubs and mud (micrite and Mg-clays). A new facies classification is proposed based on the proportion of these components within the sediments. A ternary diagram has been produced with nine facies interpreted as formed *in situ*. An additional ternary diagram using Durham's classification (grainstone, packstone, wackestone) is retained for sediments dominated by reworked facies. In addition, mudstone facies are separated into four end-members, based on mineral composition, namely calci-mudstone, dolo-mudstone, siliceous mudstone and Mg-clay mudstone. Mixed mineralogy mudstone are common.

The advantage of the proposed classification when compared to end-member facies lies in the preservation of subtle changes in the abundance of components that may have been caused by depositional/diagenetic environmental changes with possible impact on the process-based model or reservoir quality. In addition, it can be used at a range of scales and offers a means to recognize systematic changes in the vertical distribution of facies classes that can be used as a basis for analysis of cyclicity.

Using this scheme we identify two alternative facies patterns within basic cycles in the Barra Velha Formation. The mud-rich facies stacking pattern (the non-reservoir interval) occurs mainly in deeper water areas around the palaeo-high, whereas the mud-poor facies stacking pattern is more common in the shallow-water areas (the reservoir interval). Bulk chemical analysis is shown to be a valuable additional constraint on the identification of this basic cycle.

Three potential process-based conceptual models that could account for observed patterns are considered. Formation of mudstone and spherulite-rich facies with higher detrital content could arise from 1. increased fluvial detrital input to a deeper lake during wetter periods; 2. increased aeolian supply of detrital grains to a shallow lake during arid periods; or 3. decoupling from lake level but linked to spill-point elevation and/or lake stratification. Whereas in marine carbonate systems, facies variations may be interpreted largely in terms of accommodation, within alkaline lake systems the role of temporal fluctuations in lake-water chemistry may be equally or more important.

Author statement

J.P.B Gomes: Conceptualization, Methodology, Validation, Formal analysis, Investigation, Writing - Original Draft, Writing – Review & Editing, Visualization. **R.B. Bunevich.**: Validation, Investigation, Writing – Review & Editing. **L.R. Tesdeschi**: Validation, Writing – Review & Editing. **M.E. Tucker:** Conceptualization, Methodology, Validation, Writing – Review & Editing, Supervision. **F.F Whitaker**: Conceptualization, Methodology, Validation, Writing – Review & Editing, Supervision.

Acknowledgments

We acknowledge Petrobras (Brazil) for support and permission to publish this research. We thank Hilary Corlett for helping with PCA analysis and the important contributions of V. P. Wright, R. Mercedes-Martín, an anonymous reviewer and Associate Editor T. Bover Arnal.

Appendix A. Supplementary data

Supplementary data to this article can be found online at https://doi.org/10.1016/j.marpetgeo.2019.104176.

References

Arienti, L.M., Souza, R.S., Viana, S., Cuglieri, M.A., Silva, R.P., Tonietto, S.N., Paula, L., Gil, J.A., 2018. Facies Association, Depositional Systems, and Paleophysiografic Models of the Barra Velha Formation, Pre-salt Sequence – Santos Basin, Brazil. AAPG Annual Convention and Exhibition, Salt Lake City, Utah May 20–23.

Artagão, V.M., 2018. Análise estratigráfica de alta resolução aplicada aos depósitos da Formação Barra Velha, Bacia de Santos: identificação, correlação e mecanismos de controle de ciclos sedimentares. Master thesis. UERJ, Brasil (in Portuguese).

Bontognali, T.R.R., Vasconcelos, C., Warthmann, R.J., Bernasconi, S.M., Dupraz, C., Strohmenger, C.J., Mckenzie, J.A., 2010. Dolomite formation within microbial mats in the coastal sabkha of Abu Dhabi (United Arab Emirates). Sedimentology 57 (3), 824–844. https://doi.org/10.1111/j.1365-3091.2009.01121.x.

Calvo, J.P., Blanc-Valleron, M.M., RodrõÂguez-Aranda, J.P., Rouchy, J.M., Sanz, M.E., 1999. Authigenic clay minerals in continental evaporitic environments. Int. Assoc. Sedimentol. Spec. Publ. 27, 129–151.

Carminatti, M., Wolff, B., Gamboa, L., 2008. New exploratory frontiers in Brazil. In: 19th World Petroleum Congress, vol. 19 Congress Paper, Madrid.

Ceraldi, T.S., Green, D., 2017. Evolution of the South Atlantic lacustrine deposits in response to Early Cretaceous rifting, subsidence and lake hydrology. In: Petroleum Geoscience of the West Africa Margin. Geological Society, London, vol. 438. Special Publications, pp. 77–98. https://doi.org/10.1144/sp438.10.

Chaboureau, A.C., Guillocheau, F., Robin, C., Rohais, S., Moulin, M., Aslanian, D., 2013. Paleogeographic evolution of the central segment of the South Atlantic during Early Cretaceous times: Paleotopographic and geodynamic implications. Tectonophysics 604, 191–223.

Chafetz, H.S., Barth, J., Cook, M., Guo, X., Zhou, J., 2018. Origins of carbonate spherulites: implications for Brazilian Aptian Pre-Salt reservoir. Sediment. Geol. 365, 21–33. https://doi.org/10.1016/j.sedgeo.2017.12.024.

Darragi, F., Tardy, Y., 1987. Authigenic trioctahedral smectites controlling pH, alkalinity, silica and magnesium concentrations in alkaline lakes. Chem. Geol. 63 (1–2), 59–72. https://doi.org/10.1016/0009-2541(87)90074-X.

Dias, J.L., 2005. Tectônica, estratigrafia e sedimentação no Andar Aptiano da margem leste brasileira. Bol. Geociencias Petrobras 13, 7–25 (in Portuguese).

Dickson, G.W., 1966. An analysis of vendor selection: systems and decisions. J. Purch. 1, 5–17. https://doi.org/10.1111/j.1745-493X.1966.tb00818.x.

Dunham, R.J., 1962. Classification of carbonate rocks according to depositional texture. In: In: HAM, W.E. (Ed.), Classification of Carbonate Rocks, vol. 1. American Association of Petroleum Geologists, Memoir, Tulsa, pp. 108–122.

Embry, A.F., Klovan, J.E., 1971. A late Devonian reef tract on northeastern Banks Island, NWT. Bull. Can. Petrol. Geol. 19 (4), 730–781.

Erthal, M.M., Capezzuoli, E., Mancini, A., Claes, H., Soete, J., Swennen, R., 2017. Shrub morpho-types as indicator for the water flow energy – Tivoli travertine case (Central Italy). Sediment. Geol. 347, 79–99.

Falcao, L.C., 2015. Estudo Faciológico de um interval aptiano do poço SB-1 (Bacia de Santos) e sua comparação com travertinos quaternários de San Juan, Argentina. Master thesis. UFF (in Portuguese).

Farias, F.A., Szatmari, P., Bahniuk, A., França, A.B., 2019. Evaporitic carbonates in the pre salt of Santos Basin – genesis and tectonic implications. Mar. Pet. Geol. 105, 251–272. https://doi.org/10.1016/j.marpetgeo.2019.04.020.

Folk, R.L., 1959. Practical petrographic classification of limestones. Bull. Am. Assoc. Pet. Geol. 43 (1), 1–38.

Folk, R.L., 1962. Spectral subdivision of limestones types. In: In: HAM, W.E. (Ed.), Classification of Carbonate Rocks, vol. 1. American Association of Petroleum Geologists, Memoir, Tulsa, pp. 62–85.

Folk, R.L., Chafetz, H.S., Tiezzi, P.A., 1985. Bizarre forms of depositional and diagenetic calcite in hot spring travertines, central Italy. In: In: Schneidermann, N., Harris, P.M. (Eds.), Carbonate Cements. Soc. Econ. Paleontol. Mineral, vol. 36. Spec. Publ., pp. 349–369.

Herlinger, R.J., Zambonato, E.E., De Ros, L.F., 2017. Influence of diagenesis on the quality on the quality of lower Cretaceous Pre-Salt lacustrine carbonate reservoirs from northern Campos Basin, offshore Brasil. J. Sediment. Res. 87, 1285–1313. https://doi.org/10.2110/jsr.2017.70.

Kendall, A., 1977. Fascicular-optic calcite: a replacement of bundled acicular carbonate cements. J. Sediment. Petrol. 47, 1056–1062.

Kirkham, A., Tucker, M.E., 2018. Thrombolites, spherulites and fibrous crusts (Holkerian, Purbeckian, Aptian): context, fabrics and origins. Sediment. Geol. 374, 69–84. https://doi.org/10.1016/j.sedgeo.2018.07.002.

Liechoscki de Paula Faria, D., Reis, A.T., Souza Junior, O.S., 2017. Three-dimensional stratigraphic-sedimentological forward modelling of an Aptian carbonate reservoir deposited during the sag stage in the Santos basin, Brazil. Mar. Pet. Geol. 88, 676–695. https://doi.org/10.1016/j.marpetgeo.2017.09.013.

Lima, B.E., De Ros, L.F., 2019. Deposition, diagenetic and hydrothermal processes in the Aptian Pre-Salt lacustrine carbonate reservoirs of the northern Campos Basin, offshore Brazil. Sediment. Geol. 383, 55–81. https://doi.org/10.1016/j.sedgeo.2019.01.006.

Liu, K., Paterson, L., Wong, P., Qi, D., 2002. A sedimentological approach to upscaling. Transp. Porous Media 46, 285–310. https://doi.org/10.1023/A:101503111.

Lowenstein, T.K., Hardie, L.A., 1985. Criteria for recognition of salt-pan evaporites. Sedimentology 32, 627–644. https://doi.org/10.1111/j.1365-3091.1985.tb00478.x.

Madrucci, V., Araújo, C.C., Anjos, C.W.D., Spadini, A.R., 2019. Depositional paleoenvironment of authigenic magnesium clays in pre-salt of Santos Basin – Brazil. In: 16th International Meeting of Carbonate Sedimentologists, Bathurst Meeting Mallorca, pp. 152.

Manuel García Ruiz, J., 1998. Carbonate precipitation into alkaline silica-rich environments. Geology 26 (9), 843–846. https://doi.org/10.1130/0091-7613(1998)026%3c0843:CPIASR%3e2.3.CO;2.

Melo-Garcia, S.F., Letouzey, J., Rudkiewicz, J.L., Danderfer Filho, A., Lamotte, D.F., 2012. Structural modeling based on sequential restoration of gravitational salt deformation in the Santos Basin (Brazil). Mar. Pet. Geol. 35, 337–353. https://doi.org/10.1016/j.marpetgeo.2012.02.009.

Mercedes-Martín, R., Rogerson, M.R., Brasier, A.T., Vonhof, H.B., Prior, T.J., Fellows, S.M., Reijmer, J.J.G., Billing, I., Pedley, H.M., 2016. Growing spherulitic calcite grains in saline, hyperalkaline lakes: experimental evaluation of the effects of Mg-clays and organic acids. Sediment. Geol. 335, 93–102. https://doi.org/10.1016/j.sedgeo.2016.02.008.

Mercedes-Martín, R., Brasier, A.T., Rogerson, M.R., Reijmer, J.J.G., Vonhof, H.B., Pedley, H.M., 2017. A depositional model for spherulitic carbonates associated with alkaline, volcanic lakes. Mar. Pet. Geol. 86, 168–191. https://doi.org/10.1016/j.marpetgeo.2017.05.032.

Mercedes-Martín, R., Ayora, C., Tritlla, J., Sánchez-Román, M., 2019. The hydrochemical evolution of alkaline volcanic lakes: a model to understand the South Atlantic Pre-salt mineral assemblages. Earth-Sci. Rev. 102938. https://doi.org/10.1016/j.earscirev.2019.102938.

Millot, G., 1970. Geology of Clays. Springer-Verlag, Berlin 1970. 430 p.

Mizusaki, A.M.P., Petrini, R., Bellieni, G., Comin-Chiaramonti, P., Dias, J., De Min, A., Piccirillo, E.M., 1992. Basalt magmatism along the passive continental margin of SE Brazil (Campos Basin). Contrib. Mineral. Petrol. 111, 143–160. https://doi.org/10.1007/BF00348948.

Montero-Serrano, J.C., Palarea-Albaladejo, J., Martín-Fernández, J.A., Martínez-Santana, M., Gutiérrez-Martín, J.V., 2010. Sedimentary chemofacies characterization by means of multivariate analysis. Sediment. Geol. 228, 218–228. https://doi.org/10.1016/j.sedgeo.2010.04.013.

Moreira, J.L.P., Madeira, C.V., Gil, J.A., Machado, M.A.P., 2007. Bacia de Santos. Bol. Geociencias Petrobras 15, 531–549 (in Portuguese).

Muniz, M.C., Bosence, D.W.J., 2015. Pre-Salt microbialites from the Campos Basin (offshore Brazil): image log facies, facies model and cyclicity in lacustrine carbonates. In: In: Bosence, D.W.J., Gibbons, K.A., LeHeron, D.P., Morgan, W.A., Pritchard, T., Vining, B.A. (Eds.), Microbial Carbonates in Space and Time: Implications for Global Exploration and Production, vol. 418. Geological Society, London, Special Publications, pp. 221–242. https://doi.org/10.1144/SP418.10.

Perri, E., Tucker, M.E., Slowakiewicz, M., Whitaker, F., Bowen, L., Perrotta, I.D., 2018. Carbonate and silicate biomineralization in a hypersaline microbial mat (Mesaieed sabkha, Qatar): roles of bacteria, extracellular polymeric substances and viruses. Sedimentology 65, 1–33. https://doi.org/10.1111/sed.12419.

Pentecost, A., Viles, H., 1994. A review and reassessment of travertine classification. Journal Géographie Physique et Quaternaire 48, 305–314. https://doi.org/10.7202/033011ar.

Pietzsch, R., Oliveira, D.M., Tedeschi, L.R., Queiroz Neto, J.V., Figueiredo, M.F., Vazquez, J.C., Souza, R.S., 2018. Palaeohydrology of the Lower Cretaceous pre-salt lacustrine system, from rift to post-rift phase, Santos Basin, Brazil. Palaeogeogr. Palaeoclimatol. Palaeoecol. 507, 60–80. https://doi.org/10.1016/j.palaeo.2018.06.043.

Pittet, B., Strasser, A., 1998. Depositional sequences in deep-shelf environments formed through carbonate–mud import from the shallow platform (Late Oxfordian, German Swabian Alb and eastern Swiss Jura). Eclogae Geol. Helv. 91, 149–169. https://doi.org/10.5169/seals-168414.

Pollitt, D.A., Burgess, P.M., Wright, V.P., 2014. Investigating the occurrence of hierarchies of cyclicity in platform carbonates. Geol. Soc. Lond. Spec. Publ. 404, 123–150. https://doi.org/10.1144/SP404.3.

Renaut, R.W., Tiercelin, J.J., 1994. Lake Bogoria, Kenya Rift Valley: a sedimentological overview. In: In: Renaut, R.W., Last, W.M. (Eds.), Sedimentology and Geochemistry of Modern and Ancient Saline Lakes, vol. 50. SEPM Spec. Publ., pp. 101–123.

Rezende, M.F., Pope, M.C., 2015. Importance of depositional texture in pore characterization of subsalt microbialite carbonates, offshore Brazil. Geol. Soc., London, Spec. Pub 418 (1), 193–207. https://doi.org/10.1144/SP418.2.

Riding, R., 2000. Microbial carbonates: the geological record of calcified bacterial-algal mats and biofilms. Sedimentology 47, 179–214. https://doi.org/10.1046/j.1365-3091.2000.00003.x.

Rogerson, M., Mercedes-Martín, R., Brasier, A.T., McGill, R.A.R., Prior, T.J., Vonhof, H., Fellows, S.M., Reijmer, J.J.G., McClymont, E.L., Billing, I., Matthews, A., Pedley, M., 2017. Are spherulitic lacustrine carbonates an expression of large-scale mineral carbonation? A case study from the East Kirkton Limestone, Scotland. Gondwana Res. 48, 101–109. https://doi.org/10.1016/j.gr.2017.04.007.

Saller, A., Rushton, S., Buambua, L., Inman, K., Mcneil, R., Dickson, J.A.D., 2016. Pre-Salt stratigraphy and depositional systems in the Kwanza Basin, offshore Angola. AAPG (Am. Assoc. Pet. Geol.) Bull. 100, 1135–1164. https://doi.org/10.1306/02111615216.

Sartorato, A.C.L., 2018. Caracterização faciológica, estratigráfica e diagenética dos reservatórios carbonáticos da Formação Barra Velha, Bacia de Santos. Master thesis. UERJ, Brazil (in portuguese).

Souza, R.S., Arienti, L.M., Viana, S.M., Falcao, L.C., Cuglieri, M.A., Silva, R.P., Leite, C.O., Oliveira, V.C., Oliveira, D.M., Anjos, C., Amora, R., Carmo, I.D., Coelho, C.E., 2018. Petrology of the hydrothermal and evaporitic continental Cretaceous (Aptian) pre-salt carbonates and associated rocks, South Atlantic Santos basin, offshore Brazil. In: AAPG/ACE Annual Convention & Exhibition, Salt Lake City, USA.

Strasser, A., Pittet, B., Hillgärtner, H., Pasquier, J.B., 1999. Depositional sequences in shallow carbonate-dominated sedimentary systems: concepts for a high-resolution analysis. Sediment. Geol. 128, 201–221. https://doi.org/10.1016/S0037-0738(99)00070-6.

Sugisaki, R., Yamamoto, K., Adachi, M., 1982. Triassic bedded cherts in central Japan are not pelagic. Nature (London) 298, 644–647. https://doi.org/10.1038/298644a0.

Tanaka, A.P., Faria, D.L.P., Gomes, J.P.B., Souza Jr., O.G., 2018. Geological characterization and modeling of an Aptian carbonate reservoir in the Santos basin, Brazil. In: AAPG 2018 AAPG Annual Convention and Exhibition, Salt Lake City, Utah, May 20–23.

Tedeschi, L.R., 2017. Doctor of Philosophy Thesis In: Lower Cretaceous Climate Records and the Correlation Between Marine and Lacustrine Settings (Europe and South America). University of Oxford.

Terra, G.J.S., Spadini, A.R., Franca, A.B., Sombra, C.L., Zambonato, E.E., Juschaks, L.C.S., Arienti, L.M., Erthal, M.M., Blauth, M., Franco, M.P., Matsuda, N.S., Da Silva, N.G.C., Moretti Jr., P.A., D'Avila, R.S.F., De Souza, R.S., Tonietto, S.N., Dos Anjos, S.M.C., Campinho, V.S., Winter, W.R., 2010. Classificação de rochas carbonáticas aplicável ás bacias sedimentares brasileiras. Bol. Geociencias Petrobras 18, 9–29 (in Portuguese).

Tosca, N.J., Wright, V.P., 2015. Diagenetic Pathways Linked to Labile Mg-Clays in Lacustrine Carbonate Reservoirs: a Model for the Origin of Secondary Porosity in the Cretaceous Pre-salt Barra Velha Formation, Offshore Brazil, vol. 435 Geological Society, London, Special Publicationhttps://doi.org/10.1144/SP435.1.

Tutolo, B.M., Tosca, N.J., 2018. Experimental examination of the Mg-silicate-carbonate system at ambient temperature: implications for alkaline chemical sedimentation and lacustrine carbonate formation. Geochem. Cosmochim. Acta 225, 80–101. https://doi.org/10.1016/j.gca.2018.01.019.

Viera de Luca, P.H., Matias, H., Carballo, J., 2017. Breaking barriers and paradigms in Pre-Salt exploration: 562 the Pão de Açúcar discovery, (offshore Brazil). AAPG Mem. 113, 177–194.

Walker, R.G., 1992. Facies, facies models and modern stratigraphic concepts. In: Walker, R.G., James, N.P. (Eds.), Facies Models: Response to Sea Level Change. Geological Association of Canada, St. Johns, NF, pp. 1–14.

Wintsch, R.P., Kvale, C.M., 1994. Differential mobility of elements in burial diagenesis of siliciclastic rocks. J. Sediment. Reservoir 64, 349–361.

Wold, S., Esbensen, K., Geladi, P., 1987. Principal component analysis. Chemometr. Intell. Lab. Syst. 2, 37–52.

Wright, V.P., 1992. A revised classification of limestones. Sediment. Geol. 76, 177–185. https://doi.org/10.1016/0037-0738(92)90082-3.

Wright, V.P., Barnett, A.J., 2015. An abiotic model for the development of textures in some South Atlantic early Cretaceous lacustrine carbonates. In: In: Bosence, D.W.J., Gibbons, K.A., Le Heron, D.P., Morgan, W.A., Pritchard, T., Vining, B.A. (Eds.), Microbial Carbonates in Space and Time: Implications for Global Exploration and Production, vol. 418 Geological Society, London, Special Publications. https://doi.org/10.1144/SP418.3.

Wright, V.P., Barnett, A.J., 2017. Critically Evaluating the Current Depositional Models for the Pre-salt Barra Velha Formation. Offshore Brazil. AAPG Search and Discovery Article #51439.

Wright, V.P., Barnett, A.J., 2019. The Textural Evolution and Ghost Matrices of the Cretaceous Barra Velha Formation Carbonates from the Santos Basin. offshore Brazil. Facies (in press).

Yamamoto, K., Sugisaki, R., Arai, F., 1986. Chemical aspects of alteration of acidic tuffs and their application to siliceous deposits. Chem. Geol. 55, 61–76. https://doi.org/10.1016/0009-2541(86)90128-2.